

# Techno-Economic Evaluation of Various Energy Storage Technologies in the Context of the Energy Transition Using the Modelling Framework Backbone

Jan Mutke

Masterarbeit

Februar 2021

2021-MA-038



# ■ Techno-Economic Evaluation of Various ■ Energy Storage Technologies in the Context ■ of the Energy Transition Using the Modelling ■ Framework Backbone

Jan Mutke

Matr.-Nr. 108014235385

Betreuer/in:

Prof. Dr. Valentin Bertsch  
M. Sc. Leonie Plaga

■  
Masterarbeit

Februar 2021

2021-MA-038



Bochum, 19.08.2020

**Master's thesis**  
**for Mr. B.Sc. Jan Mutke**  
**Matr.-No.: 1080 1423 5385**

**Thema:** Technisch-ökonomische Bewertung verschiedener Energiespeichertechnologien im Kontext der Energiewende mithilfe des Backbone-Modells  
**Title:** Techno-economic evaluation of various energy storage technologies in the context of energy transition using the modelling framework Backbone

**Scope:**

Due to the energy transition nowadays, there is growing demand to deal with the fluctuating character of renewable energies, which comes along particularly with the integration of wind and solar power. One essential approach is to use energy storage in order to balance energy supply and demand. However, the integration of energy storage into complex energy systems leads to challenging requirements for storage technologies to meet, both technically and economically.

Backbone is a highly adaptable modelling framework for energy systems, that allows to establish custom built models for multiple purposes. The generic optimisation tool, written in GAMS, enables to investigate small- and large-scale energy systems, including the different energy sectors and providing a high temporal and spatial resolution.

The objective in this work is to evaluate different energy storage technologies in terms of upcoming technical and economical requirements within the energy transition. For this purpose, Backbone shall be used to investigate a reasonably defined area regarding energy storage. An appropriate data set is to be chosen to create models, that represent the energy storage structures in the defined network area. Since the upcoming demand for energy storage is linked to the energy transition inevitably, different future scenarios should be taken into account, for instance involving possible shares of renewables. Furthermore, the storage systems shall be analysed on an economic level. Finally, the results are to be presented in view of a successful integration of energy storage in future scenarios.

The results of the work are to be presented in a comprehensible and clear manner. Further details should be discussed with the supervisor. Two copies of the thesis as well as an electronic form remain at the Chair of Energy Systems and Energy Economics. The binding and layout are to be designed according to the specifications of the chair. The chair reserves the right to use the results for further scientific work. According to the examination regulations for the mechanical engineering program (PO 13), the duration of the master's thesis is at least four and at most six months and should not exceed 900 hours. The chair reserves the right to stop supervising the content of the scientific work if the time limit is exceeded.

**Start of work:** 20.08.2020  
**Submission of work:** 20.02.2021  
**Supervisor EE:** Prof. Dr. V. Bertsch



Prof. Dr. V. Bertsch



## Abstract

Within the energy transition, the share of renewable energies is steadily increased. In order to integrate these energies into the electricity system successfully and face their fluctuating character, energy storages may be used. Pumped hydro storages, commonly deployed, are limited by certain site restrictions. Thus, innovative storage technologies are becoming increasingly important. To explore the future potential of four innovative electrical energy storages, a model for the German electricity system in 2050 is established in Backbone. Two promising battery technologies, adiabatic compressed air energy storages and hydrogen storages are included. Furthermore, the model is investigated in terms of several CO<sub>2</sub> emission cases, and thus renewable energy (RE) shares, for the year 2050.

First significant storage deployment appears when reaching a RE share of 68 %. When reducing the allowed CO<sub>2</sub> emissions, the RE share rises and storage deployment increases exponentially. The step from 96.3 % to 100 % share of RE is striking, as it leads to a doubling of the storage power capacity. In the same step, the total system costs increase significantly, which is traced back to increasing investment costs of RE and hydrogen storage. Generally, all investigated storage technologies are utilised in at least one CO<sub>2</sub> emission case. Battery storage finds application in all CO<sub>2</sub> cases, while compressed air energy storage is only deployed at very high shares of RE. Worth highlighting is the role of hydrogen storage, which takes a consistently crucial role when approaching high shares of RE. The insights in a brief sensitivity analysis reveals that hydrogen storage keeps this dominant position when varying the capital expenditures and efficiencies of the investigated storage technologies. Apart from hydrogen storage, the other storage technologies show a partly competitive behaviour, as they provide similar functions: Both battery types show a clear correlation to photovoltaic (PV) generation and primarily shift energy from midday to evening hours. Compressed air energy storage and hydrogen storage show a correlation to both wind and PV generation and function as long term storage, that shift surplus energy all times of the year, when RE generation lacks. Additionally, a correlation between the distinct storage technologies is revealed, which leads to a more efficient storage usage.



## Kurzfassung

Im Rahmen der Energiewende gewinnen erneuerbare Energien (EE) zunehmend an Bedeutung. Um diese fluktuierenden Energien erfolgreich ins Stromnetz zu integrieren, können Energiespeicher eingesetzt werden. Dazu werden heutzutage überwiegend Pumpspeicherkraftwerke betrieben. Aufgrund einschränkender Standortkriterien sind Neuinstallationen von Speichern dieser Art begrenzt. Dadurch wächst der Bedarf an anderen Speichertechnologien. Um die zukünftige Rolle von vier innovativen Stromspeichern zu untersuchen, wird ein Modell für das deutsche Energiesystem im Jahr 2050 in Backbone erstellt. Dieses beinhaltet zwei Batterietechnologien, adiabate Druckluftspeicher und Wasserstoffspeicher. Das Modell wird in Hinsicht auf verschiedene CO<sub>2</sub>-Emissionsfälle und damit verschiedene Anteile von EE untersucht.

Erste erwähnenswerte Speicherinvestitionen zeigen sich ab einem EE-Anteil von 68 %. Bei Reduzierung der erlaubten CO<sub>2</sub>-Emissionen steigt der Anteil an EE und die Speicherinvestitionen nehmen exponentiell zu. Auffällig ist der Schritt von 96,3 % auf 100 % EE-Anteil, der sogar zu einer Verdoppelung der leistungsbasierten Speicherkapazitäten führt. Im gleichen Schritt steigen die Gesamtsystemkosten auffällig an, was auf zunehmende Investitionskosten für EE und Wasserstoffspeicher zurückgeführt werden kann. Generell kommen alle innovativen Speichertechnologien in zumindest einem CO<sub>2</sub>-Emissionsfall zum Einsatz. Die Batterietechnologien werden in allen CO<sub>2</sub>-Emissionsfällen genutzt, während Druckluftspeicher nur bei sehr hohen EE-Anteilen zum Einsatz kommen. Bei höheren Anteilen von EE nehmen Wasserstoffspeicher durchweg eine herausragende Rolle ein. Einblicke in eine kurze Sensitivitätsanalyse zeigen, dass dies auch gilt, wenn Investitionskosten und Effizienzen jeweils aller Speichertechnologien variiert werden. Die übrigen Speichertechnologien, abgesehen von Wasserstoff, stehen in einer teilweisen Konkurrenz zueinander. Der Grund dafür ist in ähnlichen Betriebsweisen zu finden: Beide Batterietypen zeigen eine deutliche Korrelation zur Photovoltaik-Erzeugung und verschieben vor allem überschüssige Sonnenenergie in die Abendstunden. Druckluft- und Wasserstoffspeicher weisen sowohl eine Korrelation zur Wind- als auch zur Photovoltaik-Erzeugung auf und fungieren als Langzeitspeicher. Diese verlagern überschüssige Energie ganzjährig in Zeiträume, in denen keine ausreichende EE-Erzeugung vorhanden ist. Außerdem zeigt sich eine Korrelation zwischen den Energiespeichern, die zu einer effizienteren Speichernutzung führt.



# Table of contents

<b>Figures</b> .....	<b>III</b>
<b>Tables</b> .....	<b>V</b>
<b>Abbreviations</b> .....	<b>VI</b>
<b>Symbols</b> .....	<b>VIII</b>
<b>Subscripts</b> .....	<b>IX</b>
<b>1. Introduction</b> .....	<b>1</b>
<b>2. Background</b> .....	<b>5</b>
2.1 Backbone network structure .....	5
2.2 PyPSA-Eur data base .....	7
2.3 Promising energy storage technologies .....	8
<b>3. Modell development</b> .....	<b>11</b>
3.1 Research approach.....	11
3.2 Assumptions .....	12
3.2.1 Basic assumptions .....	12
3.2.2 Storage technologies .....	13
3.2.3 Generation technologies .....	15
3.3 Sensitivity scenarios .....	16
3.3.1 Future load pattern.....	17
3.3.2 Investment cost.....	17
3.3.3 Efficiency .....	18
3.4 Key figures for evaluation .....	18
<b>4. Results: Energy storages in the German electricity system 2050</b> .....	<b>21</b>
4.1 Generation technologies .....	21
4.1.1 Energy mix.....	21
4.1.2 Power capacity investment .....	23
4.1.3 Curtailment of variable renewable energy.....	25
4.2 Fluctuating generation and storage deployment .....	25
4.2.1 Shift of lack and surplus generation .....	25

4.2.2	Storage communication .....	28
4.2.3	Unconventional storage charging.....	28
4.3	Energy storage technologies .....	29
4.3.1	General deployment.....	29
4.3.2	Energy to power ratio.....	31
4.3.3	Short term energy storage .....	32
4.3.4	Long term energy storage.....	34
4.3.5	Development of storage function over the CO <sub>2</sub> cases .....	37
4.4	System cost analysis .....	39
4.4.1	Total system cost.....	39
4.4.2	Investment cost.....	40
<b>5.</b>	<b>Energy storage sensitivity analysis: C97.5 .....</b>	<b>41</b>
5.1	Capital expenditures of energy storage technologies .....	41
5.2	Future load pattern.....	43
5.3	Efficiencies of energy storage technologies .....	43
<b>6.</b>	<b>Summary and conclusion .....</b>	<b>47</b>
6.1	Key findings .....	47
6.2	Discussion and outlook .....	49
	<b>Bibliography.....</b>	<b>51</b>
	<b>Appendix .....</b>	<b>57</b>

## Figures

Figure 2.1: Simplified schematic of Backbone's structure in this work. ....	5
Figure 2.2: The established network structure of Germany. The spatial resolution of the model equals ten nodes which represent the illustrated areas. ....	7
Figure 3.1: Load patterns: (a) scaled ENTSO-E pattern, (b) future load pattern considering future efficiency measures and the electrification of the heat and mobility sector. ....	17
Figure 3.2: Exemplary residual load duration curve including charging and discharging activities of energy storage. ....	19
Figure 4.1: Resulting energy mix for the investigated CO <sub>2</sub> cases.....	22
Figure 4.2: Generation share of renewable energies for the investigated CO <sub>2</sub> cases.....	23
Figure 4.3: Power capacity investments made by Backbone for the different CO <sub>2</sub> cases.....	23
Figure 4.4: Exemplary generation profile of C99.375. A week featuring a period of low VRE supply. ....	24
Figure 4.5: Development of the curtailment factor $z$ over the CO <sub>2</sub> cases. ....	25
Figure 4.6: Residual load duration curves for case C and C90 including the summed storage activities of all technologies. ....	26
Figure 4.7: Development of installed storage power capacities over the CO <sub>2</sub> cases. Values refer to discharge power capacities. ....	29
Figure 4.8: Power capacity investments made according to the different storage <i>EP</i> designs over the CO <sub>2</sub> cases. ....	31
Figure 4.9: Comparison between PV generation and LIB activities for the case C97.5: (a) PV generation pattern, (b) energy state pattern of LIB, (c) LIB charging pattern, (d) LIB discharging pattern.....	32
Figure 4.10: Comparison of energy state patterns for case C97.5: (a) VRFB, (b) PHS.....	33

Figure 4.11: Comparison between wind generation pattern and H <sub>2</sub> activities for case C97.5: (a) wind generation pattern, (b) energy state pattern of H <sub>2</sub> , (c) H <sub>2</sub> charging pattern, (d) H <sub>2</sub> discharging pattern.....	35
Figure 4.12: ACAES energy state pattern for case C97.5. ....	36
Figure 4.13: Developemnt of the key figure $t_{cyc}$ for all CO <sub>2</sub> cases. ....	37
Figure 4.14: Energy state pattern for LIB in case C85 and C100. ....	38
Figure 4.15: Cost breakdown according to the cost types over the CO <sub>2</sub> cases.....	39
Figure 4.16: Development of investment cost according to technology over the CO <sub>2</sub> cases. "Other storages" include LIB, VRFB and ACAES. ....	40
Figure 5.1: Invested storage power capacities for the storage CAPEX scenarios and the future load pattern scenario in comparison to the reference case C97.5: (a) total storage power capacity investments according to the distinct technologies, (b) deviations regarding to the reference case C97.5. ....	42
Figure 5.2: Invested storage power capacities for the efficiency scenarios in comparison to the reference case C97.5: (a) total storage power capacity investments according to the different technologies, (b) deviations with regard to the reference case C97.5. ....	44

## Tables

Table 3.1: CO <sub>2</sub> restriction cases.....	12
Table 3.2: Commodity and CO <sub>2</sub> related assumptions. ....	13
Table 3.3: Chosen <i>EP</i> designs for the investigated energy storage technologies..	13
Table 3.4: Parameter assumptions for the investigated energy storage technologies in 2050 based on several references. ....	15
Table 3.5: Technical and economic parameter assumptions for the generators in 2050.....	16

## Abbreviations

<b>Symbol</b>	<b>Description</b>
ACAES	<u>a</u> diabatic <u>c</u> ompressed <u>a</u> ir <u>e</u> nergy <u>s</u> torage
CAES	<u>c</u> ompressed <u>a</u> ir <u>e</u> nergy <u>s</u> torage
CCGT	<u>c</u> ombined- <u>c</u> ycle <u>g</u> as <u>t</u> urbine
CCGT-A	<u>c</u> ombined- <u>c</u> ycle <u>g</u> as <u>t</u> urbine <u>a</u> dvanced
CO <sub>2</sub>	<u>c</u> arbon <u>d</u> ioxide
DOD	<u>d</u> epth <u>o</u> f <u>d</u> ischarge
EEG	<u>E</u> rneuerbare- <u>E</u> nergien- <u>G</u> esetz
ENTSO-E	<u>E</u> uropean <u>N</u> etwork of <u>T</u> ransmission <u>S</u> ystem <u>O</u> perators for <u>E</u> lectricity
FLH	<u>f</u> ull <u>l</u> oad <u>h</u> ours
FOM	<u>f</u> ixed <u>o</u> peration and <u>m</u> aintenance cost
GAMS	<u>G</u> eneral <u>A</u> lgebraic <u>M</u> odeling <u>S</u> ystem
GT	<u>g</u> as <u>t</u> urbine
H <sub>2</sub>	<u>h</u> ydrogen storage
HGT	<u>h</u> ydrogen compatible <u>g</u> as <u>t</u> urbine
HS	<u>h</u> ydro <u>s</u> torage
LIB	<u>l</u> ithium- <u>i</u> on <u>b</u> attery
NG	<u>n</u> atural <u>g</u> as
OCGT	<u>o</u> pen- <u>c</u> ycle <u>g</u> as <u>t</u> urbine
OCGT-A	<u>o</u> pen- <u>c</u> ycle <u>g</u> as <u>t</u> urbine – <u>a</u> dvanced version
offwind	<u>o</u> ffshore <u>w</u> ind
onwind	<u>o</u> nshore <u>w</u> ind
param	<u>p</u> arameter
PEM	<u>p</u> olymer- <u>e</u> lectrolyte- <u>m</u> embrane electrolyser
PHS	<u>p</u> umped <u>h</u> ydro <u>s</u> torage

---

PV	<u>p</u> hoto <u>v</u> oltaic
PyPSA-Eur	<u>P</u> ython for <u>P</u> ower <u>S</u> ystem <u>A</u> nalysis – <u>E</u> urope
RE	<u>r</u> enewable <u>e</u> nergy
RFB	<u>r</u> edox <u>f</u> low <u>b</u> attery
ROR	<u>r</u> unning- <u>o</u> f- <u>r</u> iver plant
SOC	<u>s</u> tate <u>o</u> f <u>c</u> harge
VRE	<u>v</u> ariable <u>r</u> enewable <u>e</u> nergy
VRFB	<u>v</u> anadium <u>r</u> edox <u>f</u> low <u>b</u> attery

## Symbols

### Greek symbols

Symbol	Unit	Description
$\eta$	[ - ]	efficiency

### Latin symbols

Symbol	Unit	Description
$A$	[a <sup>-1</sup> ]	annuity factor
$c$	[€]	cost
$cf$	[ - ]	capacity factor
$D$	[%/d]	dissipation
$E$	[J]	energy
$EP$	[ - ]	energy to power ratio
$f$	[kg CO <sub>2</sub> /MWh]	coefficient
$P$	[W]	power
$PR$	[ - ]	power ratio
$t$	[s]	time
$z$	[%]	curtailment factor

## Subscripts

Symbol	Description
a	<u>a</u> n <u>n</u> ual
cap	<u>c</u> ap <u>a</u> city
CAPEX	<u>c</u> ap <u>i</u> tal <u>e</u> xp <u>e</u> nditure
cav	<u>c</u> av <u>e</u> rn
ch	<u>c</u> h <u>a</u> rge
CO <sub>2</sub>	<u>c</u> ar <u>b</u> on <u>d</u> io <u>x</u> ide
cyc	<u>c</u> yc <u>l</u> e
dch	<u>d</u> is <u>c</u> h <u>a</u> rge
dem	<u>d</u> em <u>a</u> nd
FC	<u>f</u> ull <u>c</u> yc <u>l</u> e
FE	<u>f</u> uel and <u>e</u> mis <u>s</u> ion
FLH	<u>f</u> ull <u>l</u> oad <u>h</u> ours
FLP	<u>f</u> uture <u>l</u> oad <u>p</u> at <u>te</u> rn
FOM	<u>f</u> ixed <u>o</u> per <u>a</u> tion and <u>m</u> ain <u>t</u> enance costs
gen	<u>g</u> en <u>e</u> ration
GT	<u>g</u> as <u>t</u> ur <u>b</u> ine
H <sub>2</sub>	<u>h</u> ydrogen storage
inst	<u>i</u> n <u>s</u> talled
inv	<u>i</u> n <u>v</u> ested
LIB	<u>l</u> ithium- <u>i</u> on <u>b</u> at <u>te</u> ry
life	<u>l</u> if <u>e</u> time
load	electric <u>l</u> oad
max	<u>m</u> ax <u>i</u> mum
NG	<u>n</u> atural <u>g</u> as

---

peak	<u>peak</u> load
res	<u>residual</u>
SD	<u>self-d</u> ischarge
st	<u>storage</u>
t	<u>t</u> ime
VOM	<u>v</u> ariable <u>o</u> peration and <u>m</u> aintenance costs
VRE	<u>v</u> ariable <u>r</u> enewable <u>e</u> nergies

# 1. Introduction

Nowadays, the climate change is one of the most heavily debated global challenges. Legally enacted in The Paris Agreement since 2015, more than 180 countries pursue to limit global warming to a maximum of 2°C, compared to pre-industrial levels (UNFCCC, 2015). As the temperature increase is strongly related to anthropogenic greenhouse gases, emissions must be reduced to prevent life threatening changes to the ecosystem, such as extreme weather patterns (IPCC, 2018). In this context, the European Green Deal was introduced, agreeing on emission reductions, especially through transforming the energy system (European Commission, 2019). However, the deployment of renewable energies (RE), such as wind and photovoltaic (PV), is linked to fluctuating generation patterns, from which a need for increased system flexibility arises (Fraunhofer ISE, 2020). Apart from demand side management, network extension or the flexibilization of conventional power plants, energy storage is one flexibility option. In times of power generation surplus, energy storages are charged, and in times of lacking generation, they are discharged, thus shifting energy production and consumption temporally. Bulk energy storage is heavily dominated by pumped hydro storage technology (PHS), both in Germany and worldwide (DOE, 2020). Yet, PHS are subject to site restrictions and social opposition, which is why future installations are likely to be limited (Sterner and Stadler, 2019, p. 510). Therefore, other energy storage technologies gain importance.

There are several studies in the literature dealing with the future role of energy storage technologies. A common approach is the investigation of the levelized cost of storage, that describes the cost per kWh of electricity discharged by a storage when considering all lifetime costs (Beuse et al., 2020; Jülch, 2016; Schmidt et al., 2019). This allows the comparison of storage technologies among each other but neglects the deployment in complex energy networks. Another common approach found, in which this work is to be classified, is the investigation of energy storages by energy system modeling. (Bussar et al., 2016; Child et al., 2019; Gils et al., 2017; Moser et al., 2020; Schill and Zerrahn, 2018). However, these models differ in their objectives, scopes, and focus:

Child et al. (2019) investigate two pathways to a CO<sub>2</sub> neutral energy system, whereby one pathway considers an independent region and the other includes an area that is connected by a transmission network. In this study, the period from 2015 to 2050 is covered in 5 year-intervals and apart from commonly investigated storage

technologies, also battery prosumers and thermal energy storages are included. Special attention is paid to the transmission grid and grid profiles. Schill and Zerrahn (2018) explore the role of energy storages in a 2050 energy system featuring high shares of RE. For this, several scenarios are explored, gradually increasing the minimum share of RE. Also, reserve provision and demand side flexibility options are considered. Two innovative storage technologies, namely hydrogen and lithium-ion batteries are included. Bussar et al. (2016) investigated the impact of variable renewable energy (VRE) deployment on storage requirements in the region of Europe, Middle East and North Africa (EUMENA region) for a fully renewable energy system in 2050. However, storage technologies are not considered in detail, as an unspecified battery type and hydrogen storage is implemented. Moser et al. (2020) provide a wide sensitivity analysis on the deployment of energy storages in 2050. In the model, which follows a least-cost approach for the energy system configuration, various innovative storage technologies are implemented. Two scenarios are observed, featuring a CO<sub>2</sub> emission reduction of 95 % and 98 % compared to 1990.

None of these studies give detailed information about the correlation of VRE generation and innovative energy storage technologies. Although Moser et al. (2020) show an example of hourly plant and storage dispatch, storages are summarized in a generic unit and the time horizon presenting a correlation is set to one exemplary week. Schill and Zerrahn (2018) presents the correlation of PHS, lithium-ion battery and hydrogen storage to VRE generation shortly. Again, an exemplary week is presented, so that correlation differences due to seasonal changes cannot be observed.

This thesis provides a detailed analysis of the correlation of four innovative electrical energy storage technologies to wind and PV generation. For this purpose, a model of the German electricity system in 2050 is designed, including lithium-ion batteries, vanadium-redox-flow batteries, adiabatic compressed air energy storages and hydrogen storages. The model is established in “Backbone”, an energy system modelling framework, which is implemented as an open source modelling tool in the General Algebraic Modeling System (GAMS). The objective function in Backbone follows a least-cost approach. (Helistö et al., 2019) Several simulations are run, each covering a two-year period beginning in 2050, so that marginal effects in the results for one central year can be reduced. Furthermore, various CO<sub>2</sub> reduction cases up to a emission neutral electricity system featuring 100% of RE share are investigated.

This work is structured in six chapters. In Chapter 2, Backbone's general structure and the data set used to model the German electricity system is explained. Furthermore, the investigated storage technologies are introduced. After that, the model development is explained in Chapter 3. The research approach, based on gradual reductions of the CO<sub>2</sub> emission, and the assumptions made are presented. As these long-term assumptions are subject to uncertainties, several sensitivity scenarios are eventually created, which focus on the impact of essential energy storage parameters. The chapter concludes with the definition of key figures in order to enable the evaluation of both energy system and the different storage technologies.

The following both chapters present and discuss the results found. In Chapter 4, the resulting electricity system is discussed in terms of the generation mix. Eventually a connection is established to the deployment of fluctuating generation and energy storages. Subsequently, the energy storage technologies are explored in detail, especially focussing on correlation patterns in terms of VRE generation. Lastly, a system cost analysis addresses the resulting system on an economic level. Chapter 5 provides the results of the sensitivity analysis. The impact of varying capital expenditure costs, deviating storage efficiencies and an alternative future load pattern on the deployment of the storage technologies is discussed. Finally, the thesis is concluded with a summary and discussion of the results and an outlook for future work.



## 2. Background

Energy system modelling allows broad investigations of complex energy system characteristics. In this work, the modelling framework Backbone is used to establish the future German electricity system in 2050 and explore innovative electricity storage technologies (Helistö et al., 2019). This chapter deals with Backbone's general structure, which is explained by means of the network established in this work. As the network is based on the PyPSA-Eur database, the data adaptation is discussed subsequently (Hörsch et al., 2018). Finally, based on upcoming technological progressions, the investigated energy storage technologies are presented.

### 2.1 Backbone network structure

In order to represent energy networks, Backbone employs grids, nodes, units and lines. A simplified scheme of the in this work created network is depicted in Figure 2.1.

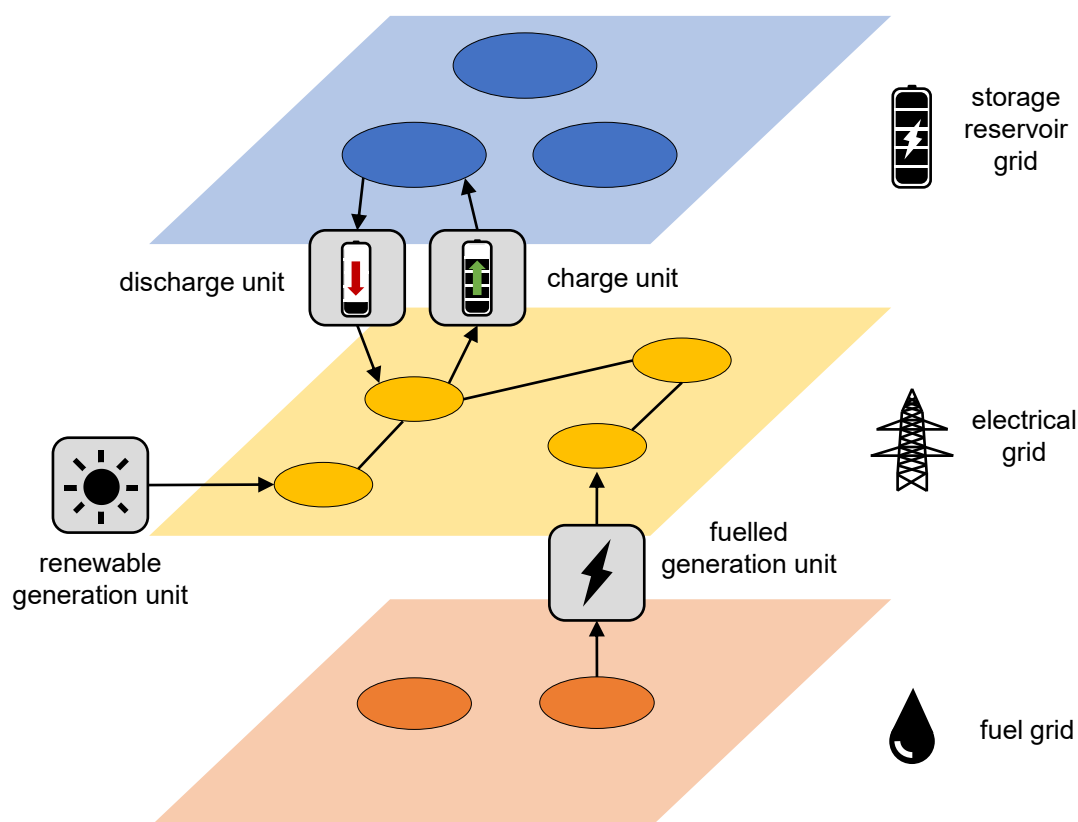


Figure 2.1: Simplified schematic of Backbone's structure in this work. Based on Helistö et al. (2019). Grids are utilised to structure energy networks in Backbone. These grids consist of nodes and lines and incorporate a common form of energy. In this work, three grids are established, namely an electrical, a fuel and a storage reservoir grid. Both the fuel and storage reservoir grid function as auxiliary networks and complement the electrical

grid. As the form of energy differs in the respective grids, a direct transfer is not permitted. Instead, the energy needs to be converted, which is handled by units. (Helistö et al., 2019)

Units are capable of producing and consuming energy at nodes and are deployed for energy conversion. While connecting nodes of different grids, they enable the energy transfer between these grids. Backbone offers multiple parameters to feature units, such as efficiency or cost quantities. Thus, units can be utilised for various purposes, when converting energy. For the given investigations, they represent dispatchable generators like gas turbines (GT), that convert fuel energy into electrical energy. Additionally, since the generation of fluctuating renewable plants such as wind turbines follows capacity factor time series instead of fuel usage, non-dispatchable generators built an own unit type, which is connected to the electrical grid only. Lastly, storage units work as converter for energy storages. While the charging process is imitated through a unit's energy consumption at an node of the electrical grid and the energy generation at a node in the storage reservoir grid, the discharge process works vice versa. The storage reservoir is modelled by nodes. (Helistö et al., 2019)

Nodes can possess states such as an energy content. Therefore, they are suitable for representing the storage energy capacity. Similar to units, various parameters allow the specification of nodes, for instance, to handle an energy capacity with an upper boundary constraint. Furthermore, nodes constitute the actual electrical network structure, whose transmission is managed by lines. These lines do not exist between storage reservoirs nodes and fuel nodes, but within the electrical grid only. Usually, energy balance is enforced in each node, so that in total the consumption must be covered by the received generation equally. This does not apply for the nodes in the fuel grid. These nodes are not energy balanced, so that dispatchable generator units are allowed to consume energy in form of fuels infinitively, but under certain prices constraints. Regarding nodes in the electricity grid, the consumption does not only come from connected units, but also through an imposed load representing a regions power demand. In this work, each unit is connected to one node in the electricity grid only. Since the nodes in the electricity grid hold spatial information, the local affiliation of the plants and energy storages is given this way. (Helistö et al., 2019)

## 2.2 PyPSA-Eur data base

PyPSA-Eur is an open model dataset of the European energy system and comprises a variety of quantities representing the area of the European Network of Transmission System Operators for Electricity (ENTSO-E) (Hörsch et al., 2018). In order to establish the network of Germany in 2050, underlying network data of the year 2013 are imported from PyPSA-Eur and eventually implemented in Backbone's structure. Figure 2.2 illustrates the resulting network, showing the spatial allocation of Germany's areas to Backbone's nodes. The PyPSA-Eur data set is discussed in the following.

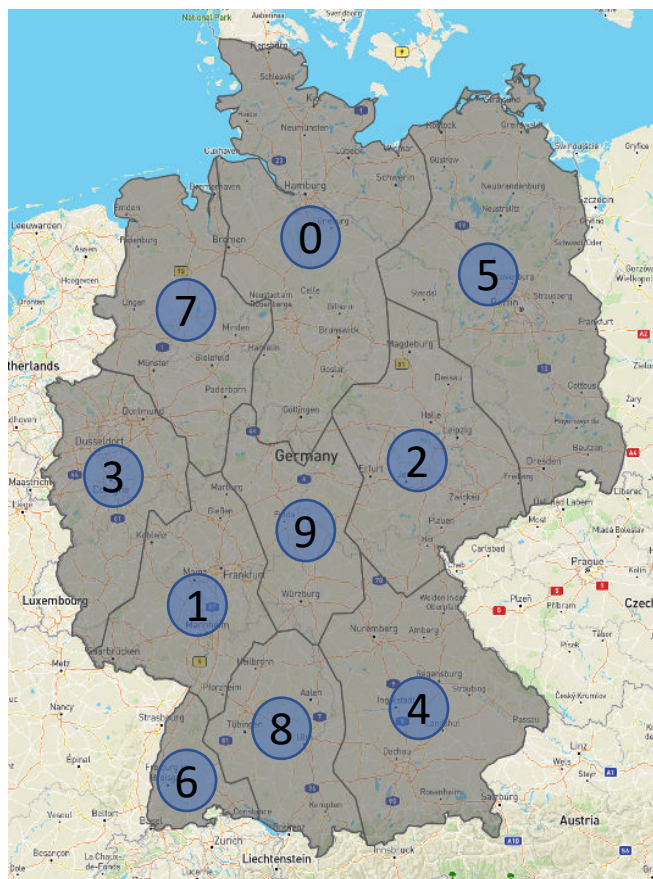


Figure 2.2: The established network structure of Germany. The spatial resolution of the model equals ten nodes which represent the illustrated areas.

The respective areas are assigned with the corresponding time series and generation capacities of 2013 found in PyPSA-Eur. The used demand data originate from ENTSO-E. (Hörsch et al., 2018) The demand is spatially distributed among the nodes with a key, whereby 60% corresponds to the gross domestic product representing the industrial demand, and 40% to the population as a proxy for residential demand. The transmission grid accounts for both high-voltage alternating current lines at levels of 220 kV, 300 kV, 380 kV and high-voltage direct current lines. Moreover, lines under or closely to construction are included as well. (Hörsch et al., 2018)

PyPSA-Eur furthermore provides generation time series and maximum installable generation capacities for renewable energies. The time series are derived from the re-analysis weather data ERA5 by the European Centre for Medium-Range Weather Forecasts for wind and hydro generators, and from the Surface Solar Radiation Data Set – Heliosat (SARAH-2) for PV generation. The potential of installable units in Germany for both wind and PV is calculated by a maximal technical potential density and a restriction factor, which regards to usable areas, competing use of land, and public acceptance issues. (Hörsch et al., 2018)

Lastly, PyPSA-Eur provides a compound database of power plants created by a power plant matching tool, that incorporates several freely accessible power plant databases (Hörsch et al., 2018). Thus, the spatial allocation of the German power plant capacities in 2013 are given. This serves as a foundation for the initial plant capacities in the developed model in 2050. The initial power plant capacities are summarized in the appendix A 1.

### **2.3 Promising energy storage technologies**

Energy storages fulfil a variety of functions, that can be broadly separated into energy balance and ancillary services (Sterner and Stadler, 2019, p. 674). Ancillary services include power applications, such as reserve provision, black start capability, voltage quality and uninterruptable power supply. Bulk energy balance gains importance with growing shares of fluctuating RE generation. In this case, energy storages are charged in times of generation surplus, and discharged in times of generation deficits. This work deals with the bulk energy balance function of storages.

Nowadays, the majority of energy storage consists of pumped hydro storages. Worldwide about 95 % of the installed energy storage power capacity is composed by PHS (DOE, 2020). However, this technology comes along with some major drawbacks. As the storage medium is water, the energy density is comparatively low and huge storage reservoirs with elevation difference are needed, standing in conflict with site restrictions and social opposition. Consequently, the future potential of PHS is limited and other technologies will likely gain significance. In this work, four emerging electricity storage technologies are investigated, that are expected to be future relevant (Schmidt et al., 2019).

Batteries are anticipated to experience a huge cost reduction in coming decades and become highly interesting as utility-scale storage option (Figgenger et al., 2020; Schmidt et al., 2017). This affects lithium-ion batteries (LIB), particularly, since the technology is deployed in various industries. For instance, the increasing usage of LIB in the transport industry is anticipated to be a crucial factor for knowledge gain and spill over to adjacent industries. LIB show comparatively high efficiencies, a low self-discharge behaviour and high energy densities. On the contrary, the deployment in various industries and the beneficial characteristics might lead to a competitive market, where the limitation of the resource lithium might play an important role (Greim et al., 2020).

Redox flow batteries (RFB) fit to large-scale storage applications, as the energy is stored by liquid electrolytes in external tanks. By decoupling battery stack and storage reservoir, RFBs can be scaled independently, which allows flexible energy to power ratios. (Lourenssen et al., 2019) Among RFBs, the vanadium redox flow battery (VRFB) is a promising flow battery, already commercially operated nowadays, and anticipated to experience significant enhancements by 2050. The drawback of a low energy density does not affect the deployment in stationary applications. (BVES, 2016b; Sánchez-Díez et al., 2021) Other battery types, for instance sodium-sulphur batteries and lead-acid batteries, might become applicable for future stationary energy storage as well. Nonetheless, these technologies are excluded in this work, as they are subject to safety and environmental issues.

Compressed air energy storage (CAES) is an alternative to PHS storage in regard to the scale and maturity. While being charged, electric energy is used to compress air, which is eventually stored in a tank or cavern. When the storage is discharged, the compressed air is heated at first, usually by the combustion of fuels, and subsequently expanded in a gas turbine, generating power. Two CAES plants are proven to work at utility scale in Huntorf, Germany and McIntosh, USA (Kaldemeyer et al., 2016). Yet, the efficiency is significantly lower than with PHS. However, through an innovative approach CAES might become more competitive in future: The adiabatic CAES (ACAES) functions basically like its origin technology, but incorporates a thermal energy storage, which captures heat occurring during the charging process when the air is compressed. When discharging, the stored heat is used to warm up the air prior to the expansion. Thereby, the deployment of fuels is substituted and the efficiency is increased remarkably. Additionally, less site restrictions and lower capital costs are expected, as no elevation difference is necessary but underground caverns

can serve as reservoir. Recently the world's first pilot scale ACAES has started operation, why it is likely that this technology will be commercially available in 2050. (Bundesamt für Energie, 2016; Geissbühler et al., 2018)

Likewise, hydrogen storage ( $H_2$ ) can be stored utilizing caverns as reservoir. As the spatial potential for cavern storage is huge and correspond with high potential wind areas in Germany, this technology is expected to play a key role for bulk energy storage in the German future energy system (Caglayan et al., 2020). The most promising technology for hydrogen production is the polymer-electrolyte-membrane electrolyser (PEM), which probably reaches an efficiency up to 80 %, experiences remarkable cost reductions by 2050 and is considered suitable for renewable energy integration (Böhm et al., 2020). Converting  $H_2$  back into power is possible with fuel cells or turbines. Common gas turbines are already partially capable of working with hydrogen. Moreover, turbine manufacturer pursue a self-imposed advancement in terms of  $H_2$  compatibility (Fraunhofer ISI, 2019). Thus, hydrogen storage is appropriate for long term storage in future energy systems.

### 3. Modell development

The third chapter presents the model development for the German electricity system in 2050. The model is based on the Backbone structure and the PyPSA-Eur data set presented in Chapter 2. It includes emerging electricity storage technologies in different designs and generation technologies according to the expected trends of the German energy system until 2050.

In a first step, the general research approach is explained. As the future development of the German energy system is likely to be marked by the energy transition, the main idea presents the reduction of CO<sub>2</sub> emissions. Eventually, assumptions are made regarding the German network, energy storages and generation technologies. Especially long-term assumptions are subject to great uncertainties. A sensitivity analysis allows insights in the impact of the assumptions on the results. Therefore, several sensitivity scenarios are created afterwards. Finally, key figures are defined, that allow the evaluation of the electricity system.

The established model is simulated over a period of two consecutive years. In this way, the evaluation can be related to a central year in the simulation period and marginal effects can be minimised, which usually occur at the beginning and the end of the simulation horizon. Input time series taken by PyPSA-Eur cover a one-year period and are used repetitively for the second year.

#### 3.1 Research approach

Since recent developments have shown that the efforts so far have not proven sufficient to limit the temperature increase as needed, the European Green Deal was enacted in 2019 calling for a zero-emission policy for 2050 (European Commission, 2019; IPCC, 2018). Germany is following this appeal by the “Erneuerbare Energien Gesetz” (EEG) (Bundesregierung, 2020). Especially, the electricity sector has a key role in this process. In 2018, about 269 million t CO<sub>2</sub> were emitted by the electricity sector in Germany, which corresponds to a reduction of 26.5% compared to 1990 (UBA, 2020). With the electrification of the heat and transport sector as part of the energy transition, it can be expected, that the electricity sector in particular will contribute the bulk share of energy related emissions. Thus, the leading research approach in this work refers to the reduction of CO<sub>2</sub> emissions in the electricity sector and different CO<sub>2</sub> cases are investigated for the established model. This allows

revealing for systems, that do not achieve the zero-emission objective and enables conclusions about the pathway to a low CO<sub>2</sub> electricity system in Germany.

Basically, eight CO<sub>2</sub> cases are explored. Beginning with no CO<sub>2</sub> restrictions at all, the allowed emissions are gradually reduced to a CO<sub>2</sub> free system. The reference emissions are based on the CO<sub>2</sub> emissions caused in the electricity sector in 1990, which equal 366 million tons CO<sub>2</sub> (UBA, 2020). Table 3.1 shows the investigated CO<sub>2</sub> cases and the accompanying emission restriction. For instance, the case C85 is associated with a CO<sub>2</sub> reduction of 85 % compared to 1990. Smaller emission reduction cases are not investigated, as the model already reaches a reduction of 81.7 % when not imposing CO<sub>2</sub> emission constraints.

Table 3.1: CO<sub>2</sub> restriction cases.

	C	C85	C87.5	C90	C92.5	C95	C97.5	C100
CO <sub>2</sub> limit [mio t/a]	-	54.9	45.75	36.6	27.45	18.3	9.15	0

## 3.2 Assumptions

Assumptions are inevitable when modelling energy systems, since these systems consist of many components that interact in complex ways. Moreover, future developments have to be estimated. This section deals with the basic assumptions made. Since energy storages are of particular interest in this work, the corresponding assumptions are attended in detail subsequently. After this, the generation technologies are addressed.

### 3.2.1 Basic assumptions

The imposed demand for overall Germany is taken from PyPSA-Eur (originating from ENTSO-E data in 2013) and scaled to 512 TWh. This value is projected under the key assumption that economic growth and energy demand will develop decoupled due to efficiency measures. (Boßmann and Staffell, 2015) The sensitivity analysis also contains a scenario considering a possible future shape of the load curve. This is further explained in subsection 3.3.1.

Germany is considered an island network and the ex- and import of power is not allowed. Additionally, the transmission network expansion is only included partially by presuming the lines currently under construction to be finished. Further investment in grid expansion is not investigated.

For simplicity's sake only CO<sub>2</sub> emissions are involved as greenhouse gas emissions. Regarding the calculation of operating costs for the gas turbines and biomass generation, the following key figures are assumed, featuring a 2050 perspective: the commodity price for natural gas (NG)  $c_{NG}$  and biomass  $c_{biomass}$ , the CO<sub>2</sub> emission coefficient for natural gas  $f_{NG,CO_2}$ , policy-imposed CO<sub>2</sub> taxes  $c_{CO_2}$ . The corresponding assumptions are summarized in Table 3.2. Biomass is considered to be emission neutral.

Table 3.2: Commodity and CO<sub>2</sub> related assumptions. (Hörsch et al., 2018; Jurich, 2016; Knaut et al., 2016)

$c_{NG}$ [€/MWh]	$c_{biomass}$ [€/MWh]	$c_{CO_2}$ [€/t CO <sub>2</sub> ]	$f_{NG,CO_2}$ [kg CO <sub>2</sub> /MWh]
33	7	76	199.5

### 3.2.2 Storage technologies

The design of energy storages varies within distinct technologies. One key figure is the discharge duration, which is equivalent to the energy to power ratio  $EP$  and is defined as follows:

$$EP = \frac{E_{cap}}{P_{dch,max}}. \quad (3.1)$$

The greater the ratio between energy capacity  $E_{cap}$  and the maximum discharge power capacity  $P_{dch,max}$ , the longer the storage is able to discharge at full load. Depending on the characteristics of the technologies, different  $EP$  are reasonable. For each technology, three  $EP$  ratio designs "S", "M" and "L" are investigated. The according ratios can be seen in Table 3.3.

Table 3.3: Chosen  $EP$  designs for the investigated energy storage technologies.

	VRFB	LIB	ACAES	H <sub>2</sub>
$EP$ (S/ML)	4 / 7 / 24	1 / 2 / 4	4 / 10 / 20	100 / 400 / 800

VRFB store liquid electrolyte in external tanks, which are theoretically freely scalable. Therefore, also the  $EP$  is mostly independently scalable. Here, VRFB are supposed as a short to medium-term storage option. ACAES store air in caverns, which is why their energy capacity depends on the respective site conditions. For this work, the  $EP$  ratios are broadly derived from the existing CAES plants. Lithium-ion batteries feature a rather fixed ratio between energy capacity and discharge power capacity. Predominantly, these ratios range between 1 to 4 according to existing storage projects

so far, which is why LIB are supposed as short term storages. (DOE, 2020) Lastly, hydrogen is deployed as long-term storage. As for ACAES, *EP* the ratio depends on the site restrictions of a certain cavern. By now, the technology is on demonstration level and the corresponding *EP* are chosen to match seasonal storage applications.

To represent the storage technologies properly, several restrictions are imposed. For ACAES and hydrogen storage, a spatial restriction is applied. Since bulk energy storage applications will necessitate huge reservoirs, salt caverns are anticipated to be the most promising possibility. Although the potential for those caverns is evaluated to be unlimited, they are subject to geographical restrictions: The majority of salt deposits is situated in the northern half of Germany (Caglayan et al., 2020; Pape et al., 2014). Therefore, ACAES and hydrogen investments are not allowed in the southern nodes 1, 4, 6, 8 (cf. Figure 2.2).

Besides, the depth of discharge (DOD) for LIB is assumed to 80 %, which is technically implemented by reducing the *EP* accordingly. The reason for this handicap is that the lifetime of LIB would be significantly reduced when using greater DOD (Sterner and Stadler, 2019, p. 302). In regard to the other storage technologies, the DOD is not constrained: On the contrary to other battery types, VRFB are capable of deep discharging (Pape et al., 2014; Sterner and Stadler, 2019, p. 319). Caverns for ACAES and hydrogen require a certain amount of cushion gas, but this is considered in the cost for the usable storage capacity (Planet, 2014).

The initial storage fleet in the model is based on the existing hydro energy storages in 2013, which are assumed to be still operatable in 2050, since common estimations let expect a lifetime lasting until 2050 (Pape et al., 2014): These storages include PHS and hydro storages without pump (HS). The according capacities and parameters can be found in the appendix A 1.

Further energy storage assumptions reflecting a 2050 perspective are given in Table 3.4. Multiple references are included, from which an average for the respective parameter is calculated after excluding outliers. Some references provide only selected parameters for a 2050 state. Values that refer to an earlier state are basically excluded, except when data is rare. Regarding the calculation of the capital expenditure costs  $c_{CAPEX}$ , only references are used, that distinguish between energy and power related costs, so that the costs for the different *EP* can be calculated.

Table 3.4: Parameter assumptions for the investigated energy storage technologies in 2050 based on several references. Technical parameter: efficiency  $\eta$ , lifetime  $t_{life}$ , power ratio between charge and discharge power capacity  $PR_{ch/dch}$ , self-discharge dissipation  $D_{SD}$ . Economic parameter: Capital expenditure costs  $C_{CAPEX}$ , fixed operation and maintenance costs  $C_{FOM}$ , variable operation and maintenance costs  $C_{VOM}$ , annuity factor  $A$ . Capital expenditure costs  $C_{CAPEX}$  are presented for the medium  $EP$  design. Hydrogen storage consists of PEM and a hydrogen compatible gas turbines (HGT).

param	unit	VRFB	LIB	ACAES	PEM	HGT <sup>1</sup>
$\eta$	[-]	0.81 <sup>2</sup>	0.93	0.70 <sup>2</sup>	0.78	0.60 <sup>3</sup>
$t_{life}$	[a]	23 <sup>2</sup>	17	45 <sup>2,4</sup>	13	28
$PR_{ch/dch}$ <sup>5</sup>	[-]	1	1	1	2	
$D_{SD}$	[%/d]	0.1250	0.0333	0.7500	0.0165	
$C_{CAPEX}$	[€/kW]	1007	383	1302 <sup>2</sup>	267	1167 <sup>3</sup>
$C_{FOM}$	[% capex/a]	2	1.4	2	2	3.1 / 1.5 <sup>3</sup>
$C_{VOM}$	[€/(MWh)]	2	2.6	1.2	0.8	4
$A$	[a <sup>-1</sup> ]	0.08871	0.10243	0.07539	0.11965	0.08239
references		(Beuse et al., 2020; Gils et al., 2017; Jülch, 2016; Moles et al., 2014; Pape et al., 2014; Schill and Zerrahn, 2018; Schmidt et al., 2019)	(Child et al., 2019; Jülch, 2016; Moles et al., 2014; Moser et al., 2020; Pape et al., 2014; Schill, 2020; Schill and Zerrahn, 2018; Schmidt et al., 2019)	(Beuse et al., 2020; BVES, 2016a; Child et al., 2019; Geissbühler et al., 2018; Jülch, 2016; Moles et al., 2014; Moser et al., 2020; Pape et al., 2014; Moser et al., 2020; Pape et al., 2014; Schill and Zerrahn, 2018)	(Böhm et al., 2020; Child et al., 2019; Gorre et al., 2019; Moser et al., 2020; Pape et al., 2014; Planet, 2014)	

### 3.2.3 Generation technologies

Within the energy transition, conventional generation technologies lose increasingly importance. In Germany, the nuclear phase out is legally enacted and the last plants will be decommissioned in the coming years (Bundesregierung, 2011). Likewise, the

<sup>1</sup> The reconversion is assumed to take place in hydrogen compatible gas turbines, which are based on the advanced CCGT in this work.

<sup>2</sup> Due to a lack of data, also values reflecting a 2030 perspective are considered.

<sup>3</sup> As Backbone provides only limited options to model the storage reservoirs separately, several according parameter are considered in the HGT:  $\eta_{cav} = 0.978$ ,  $C_{CAPEX,cav} = 400 \text{ €/kW}$ ,  $C_{FOM,cav} = 1.5 \text{ \% CAPEX/a}$ .

<sup>4</sup> Lifetime assumptions for conventional CAES are included.

<sup>5</sup> Assumption based on Jülch (2016).

coal phase out is already legally introduced and planned to be finished at least in 2038. Even more ambitious plans are discussed currently, considering the phase out until 2035. (Bundestag, 2020) For this reason, lignite, hard coal and nuclear plants are considered to be entirely decommissioned for the given model.

Hence, the initial generation capacity, which is assumed to be initially operable in 2050, is composed of open cycle gas turbines (OCGT), combined cycle gas turbines (CCGT), biomass plants and run-of-the-river plants (ROR). The initial generation capacities can be found in the appendix A 1. As power generation by oil and geothermal energy takes a neglectable share, these are not taken into account. Initial capacities for VRE are equal to zero due to a deficient data basis. Further needed generation capacities are invested endogenously by Backbone in the beginning of the simulation. This includes gas turbines, for which both OCGT-A and CCGT-A present advanced versions accounting for enhancements until 2050, and renewable energies, namely onshore wind (onwind), offshore wind (offwind), and PV generators. As for the energy storage, several references are involved. The according generator assumptions are summarized in Table 3.5.

Table 3.5: Technical and economic parameter assumptions for the generators in 2050.

param	unit	onwind	offwind	PV	OCGT-A	CCGT-A
$t_{\text{life}}$	[a]	22	24	26	26	28
$C_{\text{CAPEX}}$	[€/kW]	1051	2157	544	495	767
$C_{\text{FOM}}$	[% capex/a]	2.7	3.9	2.9	3.3	3.1
$C_{\text{VOM}}$	[€/MWh]	0.015	0.015	0.01	3	4
$A$	[a <sup>-1</sup> ]	0.09041	0.08719	0.08456	0.08456	0.08239
references		(Bussar et al., 2016; Child et al., 2019; Knaut et al., 2016; Moles et al., 2014; Moser et al., 2020; Schill and Zerrahn, 2018)	(Hörsch et al., 2018; Knaut et al., 2016; Moles et al., 2014; Moser et al., 2020; Schill and Zerrahn, 2018)	(Bussar et al., 2016; Fraunhofer ISE, 2015; Hörsch et al., 2018; Knaut et al., 2016; Moles et al., 2014; Moser et al., 2020; Schill and Zerrahn, 2018)	(Child et al., 2019; Gils, 2016; Hörsch et al., 2018; Knaut et al., 2016; Moles et al., 2014; Schill and Zerrahn, 2018)	

### 3.3 Sensitivity scenarios

Future assumptions are subject to huge uncertainties. A sensitivity analysis can provide insights in the impact of the made assumptions on the results and allows an

estimation on the resilience. However, energy systems are complex networks. As storages are the focus of this work, sensitivity investigations are conducted for the storage investment costs, storage efficiencies, and an alternative future load pattern.

### 3.3.1 Future load pattern

In terms of balancing supply and demand, the repetitive shape of the load profile contributes crucially to the need for flexibility measures. Commonly, historical load time series are scaled with future projections, as it is conducted for the base model. However, Boßmann and Staffell (2015) show that the pattern is likely to change due to the electrification of the heat and transport sector and efficiency measures. Especially the deployment of heat pumps and electrical vehicles contribute to this. For this reason, the deployment of energy storages is studied considering an additional future load pattern, which is adapted by Boßmann and Staffell (2015) for Germany in 2050. Both the future pattern and the scaled ENTSO-E profile are depicted comparatively in Figure 3.1. The large evening park for the future load pattern emerges, as the charging of the electrical vehicles is assumed to take place after working hours in this scenario.

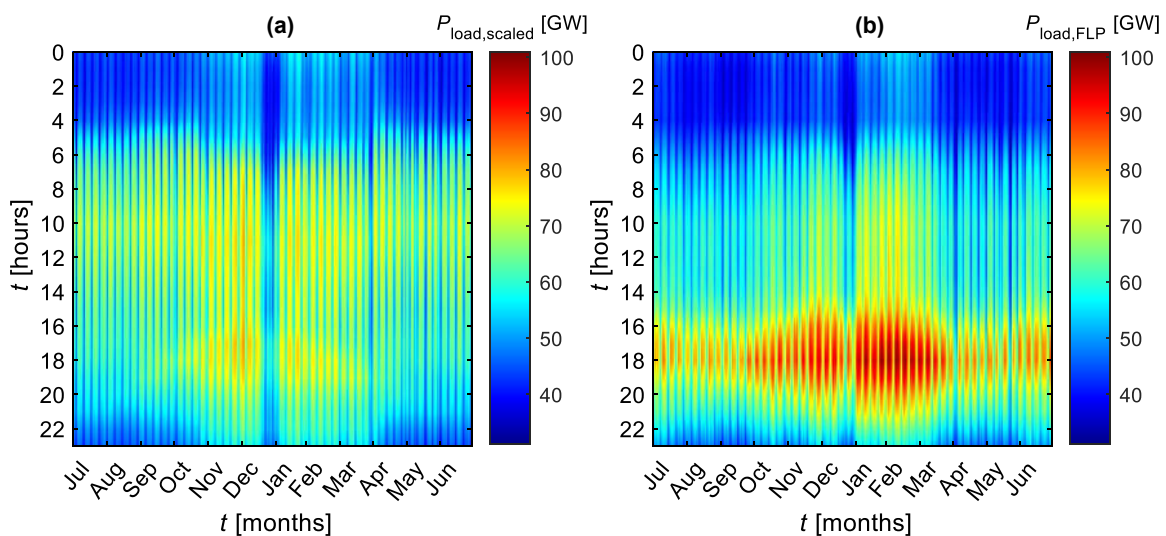


Figure 3.1: Load patterns: (a) scaled ENTSO-E pattern, (b) future load pattern considering future efficiency measures and the electrification of the heat and mobility sector. Based on eLOAD scenario “home” from Boßmann and Staffell (2015).

### 3.3.2 Investment cost

The assumed future investment costs of the storages are based on several references. Nevertheless, long-term cost projections are subject to uncertainties and may influence the competition among the storage technologies. Thus, the storage investment costs are varied in eight scenarios, in which the CAPEX cost are increased and decreased

by 20 % for a respective technology. The range of 20 % is a first assumption made in this work to provide broad insights in the impact of varying CAPEX costs.

### 3.3.3 Efficiency

Another important parameter is the efficiency, considering losses during the charge and discharge process. To explore the impact of efficiency uncertainties, for every technology a scenario is conducted, where the efficiency is increase and decreased by 2.5 %. Technically, this efficiency modification is evenly divided between the charge and discharge unit. As for the investment costs, the efficiency range of 2.5 % is a first assumptions for a broad investigation.

## 3.4 Key figures for evaluation

The following key figures are introduced for the evaluation of energy storages, renewable generators, and the overall energy system.

With growing shares of renewable energies, periods, when VRE exceed the load, become more frequent. Without having flexibility options such as storages, these energies are curtailed. Thus, a curtailment factor  $z$  is used, defined as:

$$z = 1 - \frac{E_{\text{gen},t}}{E_{\text{max},t}}, \quad (3.2)$$

whereby the actual generated energy  $E_{\text{gen},t}$  and the maximal possible energy  $E_{\text{max},t}$  that could be generated, can be expressed as:

$$E_{\text{gen},t} = \int_0^t P_{\text{gen}}(t) dt, \quad (3.3)$$

$$E_{\text{max},t} = P_{\text{inst}} * \int_0^t cf(t) dt. \quad (3.4)$$

$P_{\text{gen}}$  presents the actual power output, while  $P_{\text{inst}}$  is the installed power capacity and  $cf$  the capacity factor, which determines the maximum exploitation share for a certain VRE. Ideally,  $E_{\text{gen},t}$  and  $E_{\text{max},t}$  are identical, so that the resulting curtailment factor is zero.

The full load hours  $t_{\text{FLH}}$  give an impression of the usage of generation technologies:

$$t_{\text{FLH}} = \frac{E_{\text{gen},a}}{P_{\text{inst}}}. \quad (3.5)$$

Regarding VRE, the FLH depend on the capacity factor times series, i.e., the weather data, and the curtailment. This key figure is calculated by the yearly generated energy  $E_{\text{gen},a}$  divided by the installed power  $P_{\text{inst}}$  of a respective technology:

Another important key figure coming with fluctuating generation is the residual load  $P_{\text{res},t}$  which can be determined by:

$$P_{\text{res},t} = P_{\text{load},t} - \sum P_{\text{VRE},t}. \quad (3.6)$$

This parameter is calculated by the load  $P_{\text{load},t}$  and the sum of all fluctuating generation in a period  $P_{\text{VRE},t}$  including wind, PV and ROR generation. It shows the extent of surplus or lack of power generation when only variable renewable generation is considered. To plot the residual load over the year, a load duration curve can be used as given in Figure 3.2. The area below positive  $P_{\text{res},t}$  indicates the need for additional dispatchable generation, since VRE generation only is not sufficient. The area corresponding to negative residual loads indicates periods of surplus VRE generation, that must be basically curtailed.

When additionally plotting the charge and discharge activities of energy storages, it can be observed, that the charging process takes place in times of surplus energy and the discharge process in times when dispatchable generation must be used. This relocation of energy limits the curtailment and the additionally required dispatchable generation. The scale of the illustrated areas indicates the quantity of energy shifted.

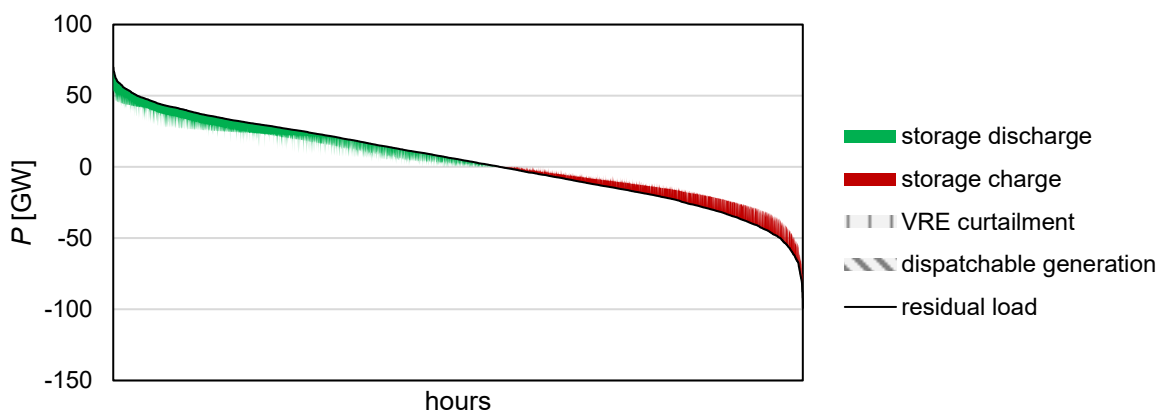


Figure 3.2: Exemplary residual load duration curve including charging and discharging activities of energy storage. Based on (Schill, 2020).

Another key figure introduced is the number of full storage cycles  $n_{FC,st}$ :

$$n_{FC,st} = \frac{E_{dch,st}}{E_{cap,st}}. \quad (3.7)$$

$E_{dch,st}$  is the total discharged energy for a respective storage technology and  $E_{cap,st}$  presents the energy capacity of the corresponding storage technology, including all *EP* designs.

When dividing the days of a year by the full cycles run by a storage in one year, the days needed for one full storage cycle  $t_{cyc,st}$  are obtained:

$$t_{cyc,st} = \frac{365}{n_{FC,st.365}}. \quad (3.8)$$

Note, that  $t_{cyc,st}$  describes an average value. It indicates, how many days pass until one full storage cycle is completed, i.e. a storage is fully charged and discharged once. However,  $t_{cyc,st}$  does not represent the real days per cycle, as it is only an average value. More precisely, energy storages are not always charged or discharged entirely, and also partial cycles are run. Nevertheless,  $t_{cyc,st}$  helps with the quantitative classification in terms of temporal characteristics of short and long-term storages.

## 4. Results: Energy storages in the German electricity system 2050

Several simulations were conducted in Backbone<sup>6</sup>. In this chapter, the evaluation of the established model for the German electricity system in 2050, including chosen electrical energy storages, is presented. In this regard, it is firstly dealt with the generation technologies. Before discussing the deployment of the energy storage technologies, the residual load characteristics are addressed. Eventually, the energy storage technologies are investigated concerning their operational behaviour and correlation to VRE. In order to investigate the system on an economic level, a system cost analysis is conducted finally.

To exclude marginal effects occurring at the beginning and the end of the simulation period, the following results refer to a central year within the simulation horizon. This equals a period from July to June, or the timestep from 4380 to 13139. An exception concerns the system cost analysis, which refers to the entire simulation period.

### 4.1 Generation technologies

In this section, the resulting energy mix for the established model is investigated, while comparing the results for the different CO<sub>2</sub> constraints. The occurring trend is explained afterwards by revealing the generation investments made. Lastly, the curtailment of PV, onshore and offshore wind generation is compared.

#### 4.1.1 Energy mix

The resulting energy mix for the respective CO<sub>2</sub> cases is shown in Figure 4.1. When not imposing a CO<sub>2</sub> constraint (case C), this results in CO<sub>2</sub> emissions of 66.87 million t CO<sub>2</sub>. Case C represents the cost optimal energy mix and equals a reduction of 81.7 % compared to the CO<sub>2</sub> emissions in the electricity sector in 1990. Consequently, the CO<sub>2</sub> limit is achieved in every other case with imposed CO<sub>2</sub> restriction.

Basically, two trends can be observed. With increasing CO<sub>2</sub> restriction, the conventional generation share, mainly consisting of CCGT generation, declines and is substituted by VRE. Up to the case C97.5, onshore wind and PV generation increase

---

<sup>6</sup> used program versions: Backbone - <https://gitlab.vtt.fi/backbone> (branch "dev", commit 24.06.2020); GAMS system 32.2.0; PyPSA-Eur 0.2.0

in a similar pattern, beginning with a generation share of 10.2 % and 12.5 % in case C, and ending in case C97.5 with 24.8 % and 27.3 %, respectively. Offshore wind generation also rises from 33.2 % in case C, finding its maximum with 42.4 % in case C95.

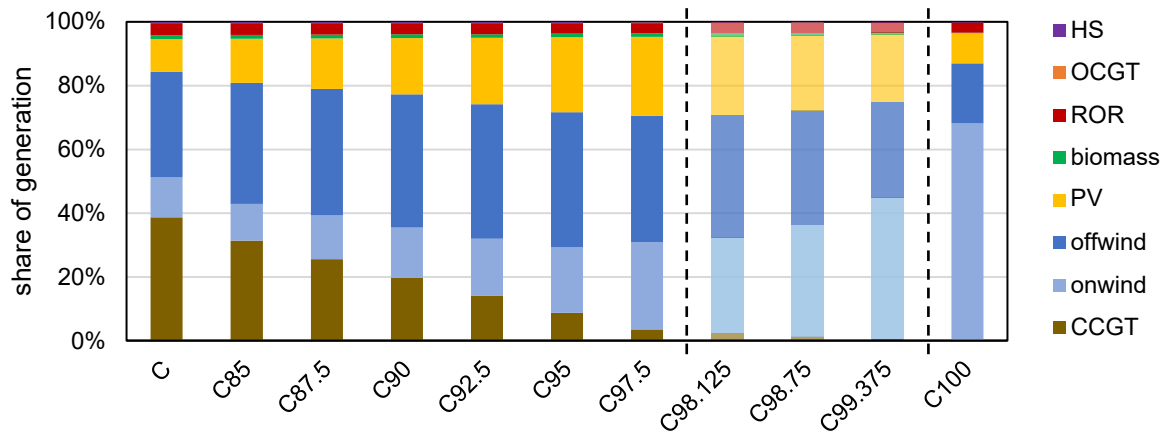


Figure 4.1: Resulting energy mix for the investigated CO<sub>2</sub> cases.

From C97.5 to C100 a contrary trend can be seen: When following the regular step size of 2.5 % regarding the increasing CO<sub>2</sub> restriction, a striking leap occurs. In contrast to the previous trends, both PV and offshore wind generation share declines to about 9,4 % and 18,8 %, respectively. Onshore wind generation grows significantly, finally taking a share of 68 % in C100. To reveal this course in detail, three additional intermediate cases are presented, showing a turnaround at C97.5. The reason for this turnaround is further investigated in the following subsection 4.1.2.

The generation share of hydro storage, OCGT, ROR and biomass makes a small share and runs consistently in all cases. What moreover should be noted is, that the total generated energy rises from 513 TWh to 606 TWh from C to C100, which is due to the increasing usage of storages and the accompanying dissipation energy. The load within the CO<sub>2</sub> cases remains the same.

Of further interest is the development of the renewable generation share, which is shown in Figure 4.2. The unrestricted CO<sub>2</sub> case results in a RE share of 61.1 %. This might seem high, but is a reasonable result, as no other conventional generators apart for GT are operated, and technology advancements until 2050 are considered. While the CO<sub>2</sub> restrictions increase, the RE share rises steadily featuring a gentle right bent curve. Finally, the RE share reads 100 % in the CO<sub>2</sub> neutral case C100.

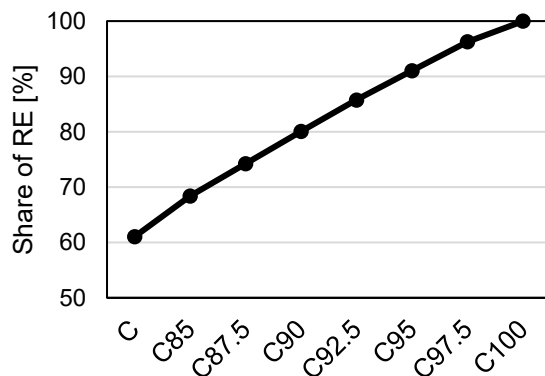


Figure 4.2: Generation share of renewable energies for the investigated CO<sub>2</sub> cases.

#### 4.1.2 Power capacity investment

To reveal the cause of the turnaround at C97.5 mentioned above, a look at the generation capacity investments made by Backbone is helpful. These are shown in Figure 4.3.

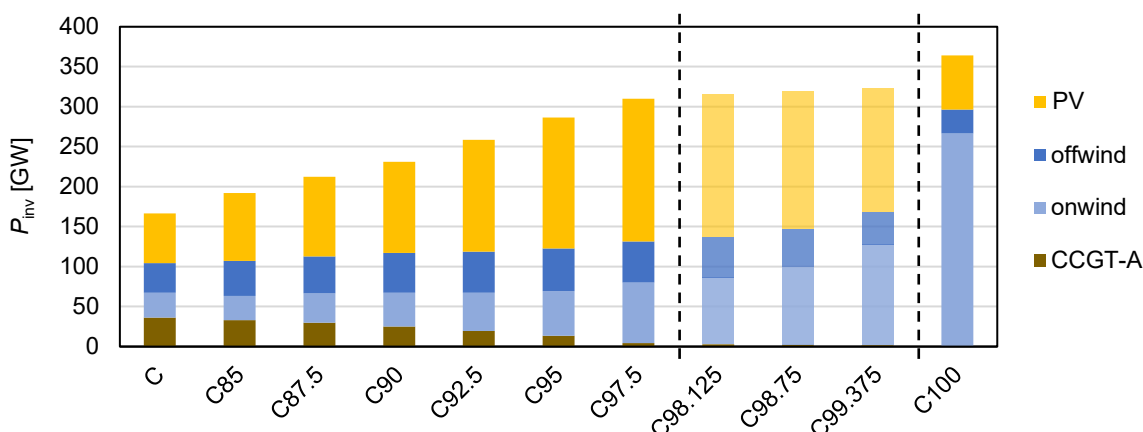


Figure 4.3: Power capacity investments made by Backbone for the different CO<sub>2</sub> cases.

While investment in gas turbine (GT) capacities decline due to the gradually increasing CO<sub>2</sub> emission limit, the total power capacity grows. As for the energy mix a similar course is found, showing, that VRE replace the GT investments. Furthermore, the invested capacities of all VRE increase to case C97.5, whereby PV stands out significantly. This cannot only be traced back to the slightly growing demand due to the storage dissipation, but also to full load hours. Whilst PV has full load hours in a range of 850 h/a, onshore wind has about 2100 h/a, and offshore wind generators 4500 h/a. The smaller the respective full load hours are, the greater the investments must be to substitute dispatchable generators. After C97.5, the PV and offshore wind capacity investments decrease, being replaced by onshore wind generators.

Two conspicuous features are found while this turnaround takes place. Firstly, increasingly more nodes, that provide decent solar radiation reach their maximal PV potential. So, in C97.5 five of six nodes situated in Germany's southern half have installed their PV maximum. Secondly, beginning from case C97.5 the spatial distribution of the remaining GT investments is striking, as these investments are only made in nodes with PV deployment. When observing the deployment of GT generation from C97.5 to C100, all capacities are used for balancing PV generation in periods of low VRE supply only. An example is illustrated in Figure 4.4, including a generation breakdown and the summed energy storage discharge (ES dch).

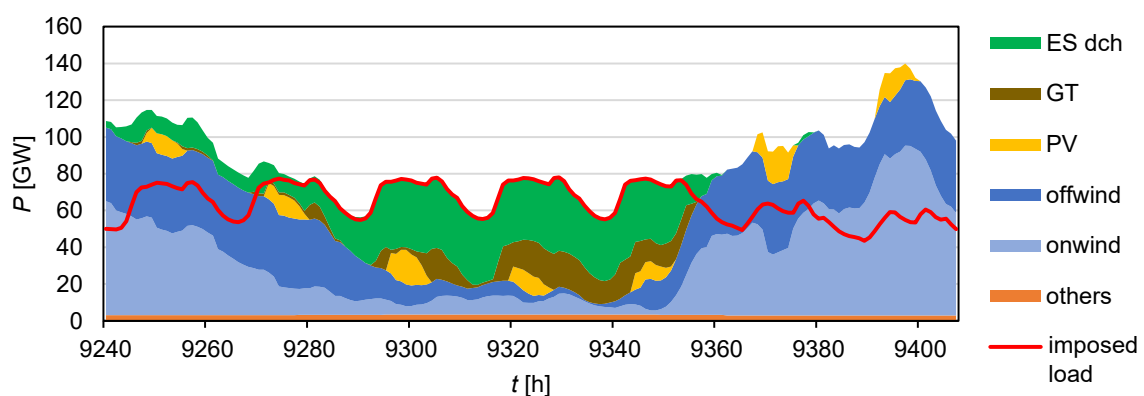


Figure 4.4: Exemplary generation profile of C99.375. A week featuring a period of low VRE supply.<sup>7,8</sup> Both the daily pattern of PV and times of low wind and solar supply in general lead to a high need of balance. In terms of cost, this is ideally covered by GT. However, the more GT deployment is restricted by limited CO<sub>2</sub> emissions, the more other options must cover the load in “dark doldrum” periods. Onshore wind units are significantly more deployed for increasing CO<sub>2</sub> restrictions as seen above. Therefore, it can be concluded that the combination of onshore wind and storages is a better option for covering great “dark doldrum” periods than using PV. This seems reasonable as more onshore wind leads to a great surplus energy due higher FLH than for PV. Moreover, onshore wind also provides generation in the night. The reason why offshore wind is not used instead might be linked to differing weather patterns of on- and offshore wind. In case C100, where no GT is in usage anymore, all remaining PV investments match up spatially with the hydrogen restricted nodes. Apparently, PV stays only cost competitive when hydrogen storage cannot be used in combination with onshore wind.

<sup>7</sup> discharging in times of surplus is discussed in subsection 4.2.2.

<sup>8</sup> „others“ include ROR, HS, and biomass generation.

### 4.1.3 Curtailment of variable renewable energy

The total VRE curtailment for the evaluated year is presented in Figure 4.5. Although the installed capacities of VRE rise with increasing CO<sub>2</sub> limitation, the curtailment for all VRE generators stays relatively low until C99.375. Both sorts of wind show a similar trend and stay in a range of 2.5 % and 7 %. An exception is C100, where onshore wind curtailment rises to 24.8 %, while offshore wind curtailment reads 16.3 %. This is related to the striking rise of wind capacities, seen in the previous subsection, and thus larger amounts of surplus energy. PV experiences no exceptional curtailment over all cases and does not exceed 0.2 %. The reason for the low curtailment level of the VRE in the most CO<sub>2</sub> cases lies in the usage of energy storages and can be understood when observing the residual load duration curves. These are discussed in the following section.

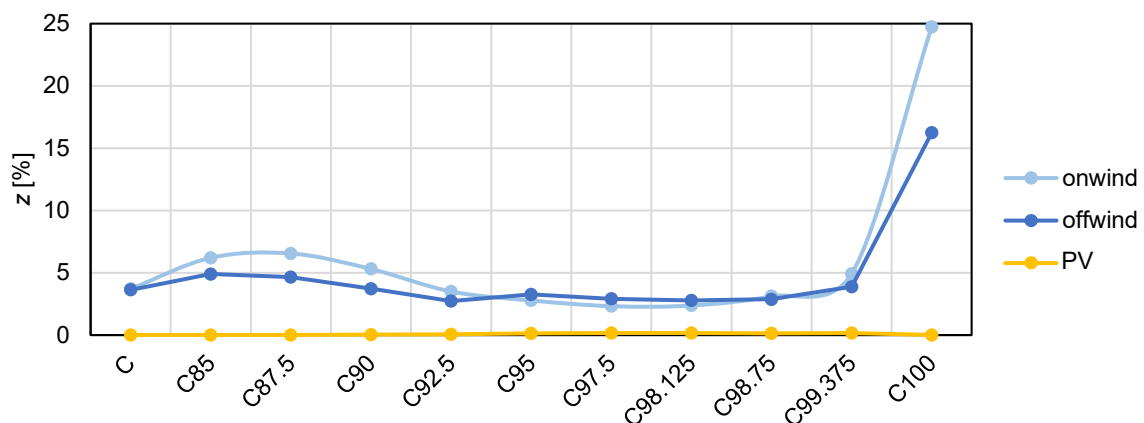


Figure 4.5: Development of the curtailment factor  $z$  over the CO<sub>2</sub> cases.

## 4.2 Fluctuating generation and storage deployment

This section deals with the fluctuating character of VRE in relation to the general function and deployment of energy storages. As introduced in section 3.4, residual load duration curves provide information about the lack and surplus generation of VRE, why this tool is the base for the following evaluation.

### 4.2.1 Shift of lack and surplus generation

Two residual load duration curves for the cases C and C90 are comparatively depicted in Figure 4.6. Additional illustrations can be found in the appendix A 2 showing the development for more CO<sub>2</sub> cases.

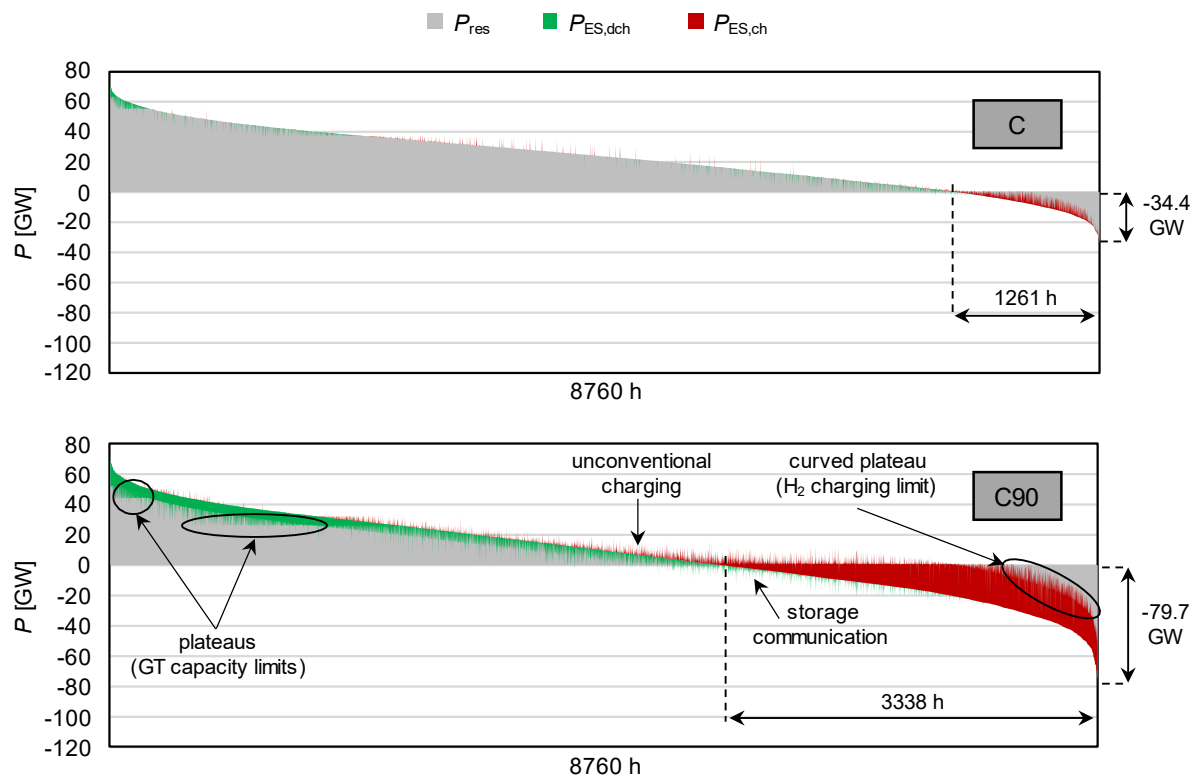


Figure 4.6: Residual load duration curves for case C and C90 including the summed storage activities of all technologies.

Basically, a shift of the lack and surplus areas takes place. With increasing CO<sub>2</sub> restriction, VRE gain capacities as shown in subsection 4.1.2. Consequently, periods of surplus increase and periods, when VRE generation falls below the load, become rarer. So, the fluctuating generation exceeds the imposed load only for 1261 h in case C, but for 3338 h in C90. Periods of lacking VRE supply make the contrary. Concurrently, the minimum peak on the surplus side decreases noticeably from -34.4 GW in case C to -79.7 GW in case C90. The peak on the left-hand side only decreases slightly, as the greater VRE capacities do not provide a remarkable greater generation in dark doldrums periods.

Consequently, the energy that would have to be curtailed grows, and required dispatchable generation decreases. However, as seen in Figure 4.5, the curtailment stays on a comparatively low level. This is due to the growing deployment of energy storages. During periods of surplus, storages are charged, thus reducing the VRE curtailment. On the side of lacking VRE generation, storages are discharged, thus decreasing the need for dispatchable generation. Strikingly, the charged energy increases from case C to C90, which is seen from the red area. Therefore, the curtailment is kept on a low level. Yet, the entire surplus VRE energy is never charged, what can be observed from the remaining grey area in the surplus area and is also

indicated by the curtailment factor  $z > 0$ . This is because storages reach either their energy or power capacity limit, and further storage investments would be less economic than simply curtailing the remaining surplus energy. Hydrogen as a long-term storage technology reaches predominantly its power capacity limit. This is reflected by the curved plateau, marked in the C90 surplus area. An exception regarding the curtailment development is seen in case C100, where the increased onshore wind capacity investments lead to a huge VRE surplus and greater curtailment than observed in all other cases. This can also be seen in the residual load duration curve for C100 (appendix A 2). Charging activities cover a smaller area, and at the same time surplus hours rise to 5102 h, whereby the surplus peak reads even 245.5 GW.

Accompanying with rising charging activities for increasing the CO<sub>2</sub> limits, the discharged activities rise as well. From case C to C90 discharging predominantly happens in times of high residual load. When CO<sub>2</sub> emissions are further restricted, discharge activities increase and stretch along all positive residual loads. Finally, in C100 almost all lacking generation is provided by energy storages.

Furthermore, several aspects in the given residual load duration curves are striking. These are marked in the C90 curve. There are several even plateaus on the side of positive residual load. These result from generation capacity limits of non-dispatchable plants, gas turbines, particularly. In times of high residual load, namely when both low VRE generation is available and there is a high load, gas turbine capacities are exhausted, and the entire remaining demand must be provided by storages. For economic reasons, the deployment of the storage technologies and gas turbine technologies compete gradually, so that several plateaus can be seen. For instance, a plateau can be traced back to the point where OCGT is not cost competitive against certain storage deployment, but CCGT capacities are entirely exhausted, as they are cheaper.

Lastly, an unconventional behaviour of storages can be recognised, which stands out through the peaks lying outside of the grey marked areas: While here charging takes place in some periods of positive residual load, i.e., when VRE generation is actually lacking, discharging can also be found in periods of generation surplus, where sufficient supply should be already given. Moreover, charging activities, that exceed the surplus area, and discharging activities, that exceed the positive residual load are

found. This unconventional storage behaviour occurs due to certain capacity limits and is divided into storage communication and unconventional storage charging. Both is discussed in the following subsections.

#### **4.2.2 Storage communication**

Unconventional discharging can be described as storage communication: In lasting periods of surplus VRE generation, short term storage reaches its energy capacity limit easily. Long-term storage, especially hydrogen, is rather limited by its charging power capacity and does not reach its energy capacity often. In order to ensure a maximum of energy captured in lasting surplus periods, short term storages do not stay idled when they are already fully charged. Instead, they support the hydrogen charging. So, short-term storages discharge when a surplus exists, that yet falls below the H<sub>2</sub> charging capacity. The short-term storage discharging is then used to keep H<sub>2</sub> charging as high as possible. Subsequently, when VRE surplus exceeds the H<sub>2</sub> charging capacity, short term storages can be charged again until they hit their energy capacity anyway. This way, a maximum amount of energy can be captured over lasting surplus periods. An exemplary week showing this effect is given in the appendix A 5.

#### **4.2.3 Unconventional storage charging**

The unconventional charging appears for two reasons. Firstly, it occurs in accordance with the storage communication as a mirror effect. When additional discharge generation is provided by short-term storages, hydrogen charging can exceed the regular VRE surplus, which ends up in the charging peaks exceeding the actual VRE surplus.

Secondly, unconventional charging is found when storages are charged with gas turbines. This might seem pointless due to the resulting efficiency losses. However, it makes sense, if the GT reach their generation capacity limit subsequently, and storages have been run empty because of previous low VRE supply. Before the GT hit their generation limit, they charge the empty storages, so that these can eventually provide the lacking generation. In several conditions, short-term storages are even used for unconventional charging, when H<sub>2</sub> storage is not empty and could be operated. This is because the long-term energy shift by H<sub>2</sub> would cause greater losses (e.g.,  $\eta_{H_2} \approx 47\% > \eta_{GT+LIB} \approx 54\%$ ). If the remaining load after exhausting GT capacities is too great to be covered by the LIB, which are primarily used due to the highest

efficiency, the economically next storage technology is deployed for conventional charging. The order in this regard apparently follows the storage efficiencies. Lastly, even hydrogen can be charged by GT in times when all storages, including H<sub>2</sub> storage itself, are run empty and the eventual residual load exceeds the GT capacities by far. An exemplary week showing unconventional charging with LIB is given in the appendix A 6.

### 4.3 Energy storage technologies

As seen beforehand, storages take an increasingly crucial role by shifting energy from periods of surplus to periods of low VRE supply. This section provides further information about the deployed storage technologies.

#### 4.3.1 General deployment

Figure 4.7 presents the development of the resulting storage power capacities in terms of the respective technology shares. Moreover, the share of the renewable energy generation is depicted. PHS capacities remain the same as no investments are allowed.

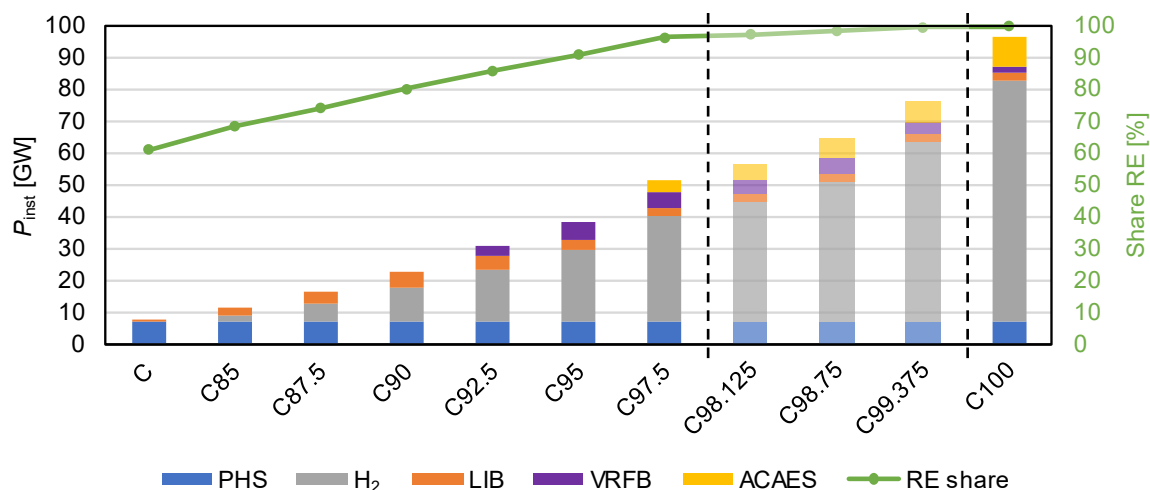


Figure 4.7: Development of installed storage power capacities over the CO<sub>2</sub> cases. Values refer to discharge power capacities.

While the share of RE rises consistently, the total energy storage power capacities increase exponentially. Especial growth is found when approaching C100, why several intermediate cases are additionally depicted.

When not imposing a CO<sub>2</sub> restriction, the need for additional storages is apparently small. So, case C results in 7.8 GW of installed storages, whereby 7.1 GW consist of initially existing PHS capacities. In this case, the RE share is 61.1%. With increasing

CO<sub>2</sub> restriction, the RE share and the storage deployment rise, ending up in C97.5 with 51.2 GW of installed storage power capacities and 96.3 % RE generation share. From this point the deployed storages enlarge significantly. While the share of RE generation gains the remaining 3.7 % to the CO<sub>2</sub> neutral system C100, the installed power capacity of storages almost doubles to 96.4 GW.

This huge increase is mostly related to more investments in hydrogen storage. When comparing this trend to the results found in the previous sections, this leap seems reasonable. In the same step from C97.5 to C100, onshore wind investments increase hugely as well. Consequently, periods of surplus and the total surplus energy over the year rises, as seen in the load duration curves. H<sub>2</sub> storage has a smaller efficiency than short-term storage such as LIB but provides large energy capacities which are needed to shift as much surplus energy as possible. This is especially true for the case C100, where no GT are deployed anymore and lacking VRE generation must be covered by storages mainly.

In terms of the distinct storage technologies the following trends become clear. As no further investments in PHS are allowed, the according capacity stays constant, so that the PHS power capacity share decreases from over 90 % in case C to 7.4 % in the CO<sub>2</sub> neutral case C100. H<sub>2</sub> is installed in case C85 for the first time, reading 1.9 GW or 16.4 %, respectively. Afterwards H<sub>2</sub> experiences the greatest increase, making the most dominant technology in terms of installed power capacity from C90. Finally, H<sub>2</sub> ends up with 75.5 GW, or a capacity share of 78.4 % in C100. The other technologies, namely LIB, VRFB and ACAES, show a partially competitive course. The LIB is the first storage technology, in which is invested in. This might be related to the comparatively low investment costs and high efficiency. So, 0.7 GW LIB are installed in case C, making the complementary share to PHS. After finding its maximum share of 22.1 % in C90, reading 5 GW, the LIB deployment declines and it is partially replaced by VRFB. First VRFB and ACAES investments take place in C90 and C97.5, respectively. The maximal VRFB share and power capacity is found in C95 equalling 9.4 % and 5.5 GW. Eventually, ACAES are introduced in C97.5 and replace LIB and VRFB storages in some extent as well. Finally, ACAES ends up with 9.1 GW or 9.5 % in C100. A hint at the reasons for this competitive behaviour can be revealed when investigating the specific *EP* investments.

### 4.3.2 Energy to power ratio

For H<sub>2</sub> no noticeable trend regarding the *EP* is found. The designs “H<sub>2</sub> S” (*EP* = 100) and “H<sub>2</sub> M” (*EP* = 400) are mainly deployed, and the corresponding investments increase while the allowed CO<sub>2</sub> emissions are reduced. The design “H<sub>2</sub> L” (*EP* = 800) is only used in C95 and C97.5 and to a small extent.

The power capacity investments according to the *EP* and the other storage technologies are depicted in Figure 4.8. Basically, it can be observed that with increasing CO<sub>2</sub> limitation gradually more energy storage technologies with greater *EP* are used. This is seen within and among the storage technologies. LIB investments in case C comprise only the “LIB S” design (*EP* = 1). In case C85, this design is replaced by “LIB M” (*EP* = 2). In case C90, the increase of “LIB L” (*EP* = 4) leads to stagnating investments of “LIB M”. This behaviour generally continues with “VRFB M” (*EP* = 7) and “ACAES L” (*EP* = 24), which are firstly used in C92.5 and C97.5, respectively.

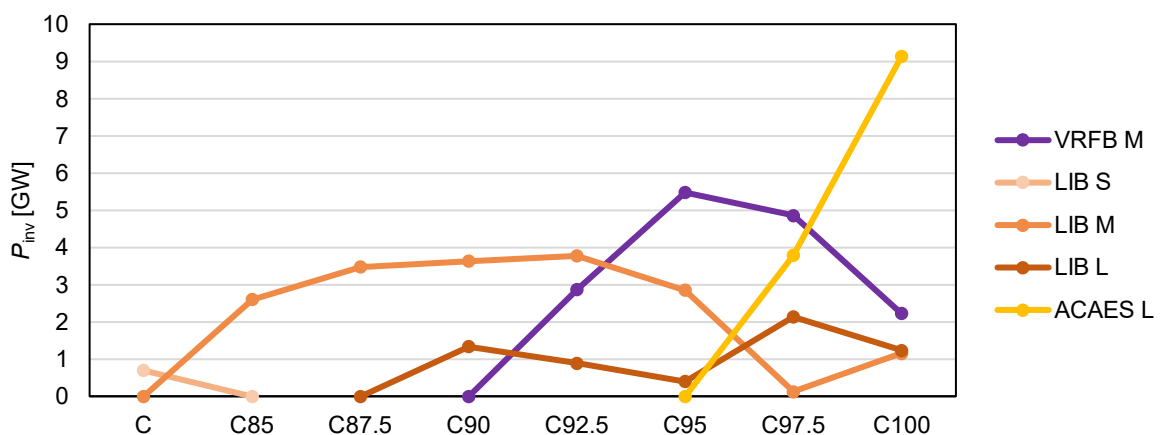


Figure 4.8: Power capacity investments made according to the different storage *EP* designs over the CO<sub>2</sub> cases.<sup>9</sup>

It can be suspected that this development is related to the rising surplus VRE generation as shown in subsection 4.2.1. The greater the amount of surplus energy is, the more cost competitive storage technologies with larger energy capacities become. In the beginning, LIB are sufficient for handling decent amounts of energy shifting. Subsequently, greater storage reservoirs gain importance, which is why the VRFB and afterwards the ACAES is used. Note, that no investments are made in those designs not shown here, since they are apparently not cost beneficial in contrast to the used storage designs. This concerns the technology designs “ACAES S”, “ACAES L” and “VRFB L”.

<sup>9</sup> VRFB S power capacity investments not shown for clarity and due to low investments.

### 4.3.3 Short term energy storage

The function of the investigated energy storages becomes clear when observing their correlation to the VRE generation. Figure 4.9 depicts the PV generation pattern comparatively to the energy state pattern, the charging pattern and the discharging pattern of LIB over the daily and yearly progression.

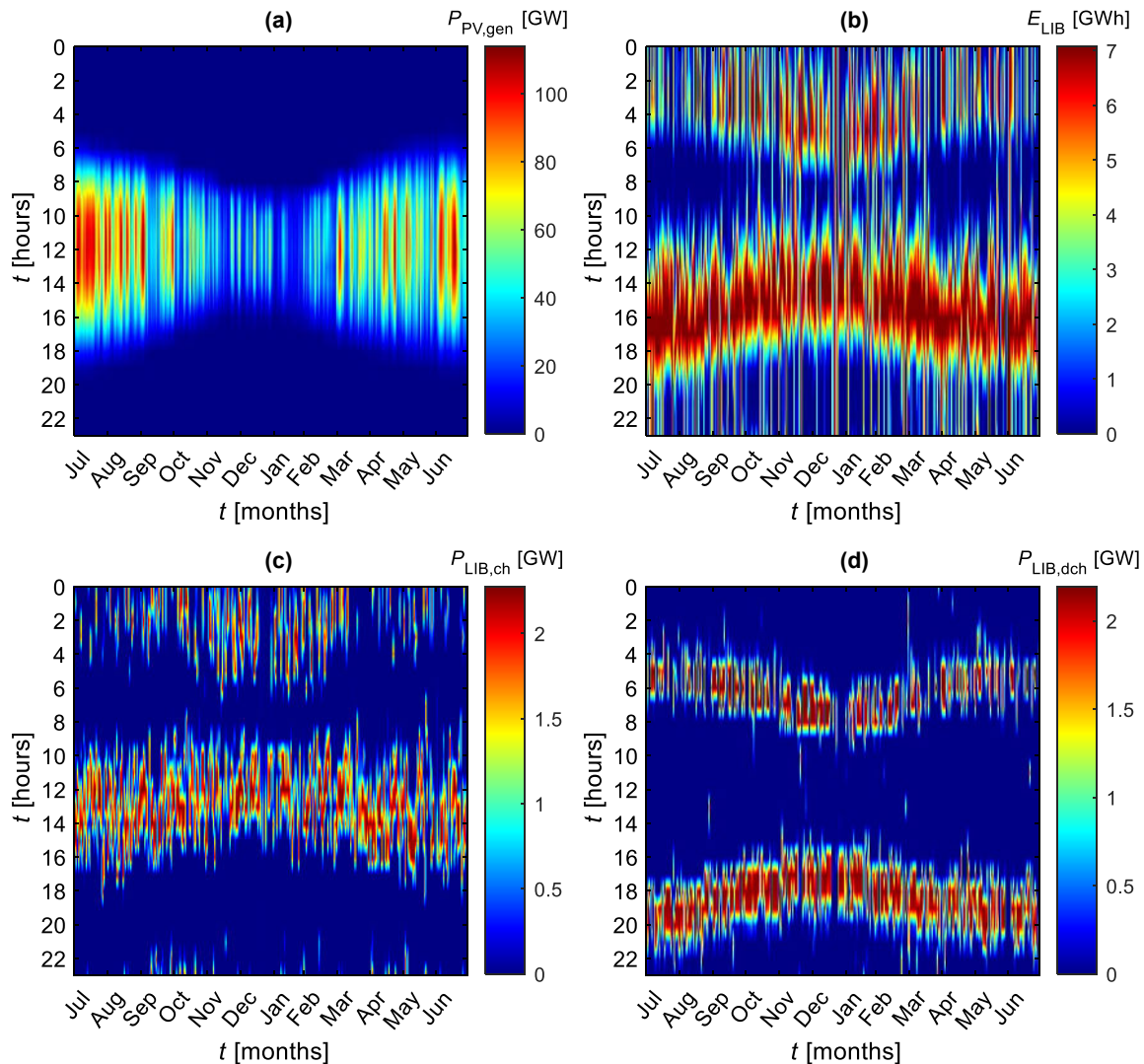


Figure 4.9: Comparison between PV generation and LIB activities for the case C97.5: (a) PV generation pattern, (b) energy state pattern of LIB, (c) LIB charging pattern, (d) LIB discharging pattern.

Obviously, PV generation takes place by day and finds its peak at midday when solar radiation becomes greatest. Furthermore, a decline can be seen due to the seasons, whose minimum is found around January.

The lion share of LIB charging occurs in the midday hours showing a high correlation to the PV generation. The gentle bend from October to March in the afternoon hours is linked to the shorter periods of sunshine in winter times. The corresponding bend

cannot be found in the morning hours (8 - 10 o'clock), since other storage technologies are charged first. Secondary charging activities are revealed in nightly hours, broadly spread between 22 and 6 o'clock all over the year. These appear when the load is on a low level and surplus wind generation is available. According to greater wind volumes in winter times, the nightly LIB charging activity becomes largest from October to February.

The discharging pattern optically circles the PV generation pattern by day. So, bulk discharge takes place in the evening hours, when the load is high and no PV is available, and in early morning hours, when the load increases and the PV generation is small as well. The bent character is linked with seasonal appearances.

The resulting pattern for the LIB energy state suits to the described behaviour yet gives further revealing. The clearly seen dark red plain coloured areas indicate the energy capacity limit for LIB, mainly occurring after the PV peak. Therefore, it can be concluded that LIB are predominantly limited by their energy capacity. Moreover, vertical-coloured lines are found that stretch along all hours of a day. This indicates a lasting energy state for at least one day, thus shifting energy inter-days.

Similar patterns are found for VRFB and PHS, whose energy state patterns are exemplary illustrated in Figure 4.10. The according charging and discharging patterns are depicted in the appendix A 3.

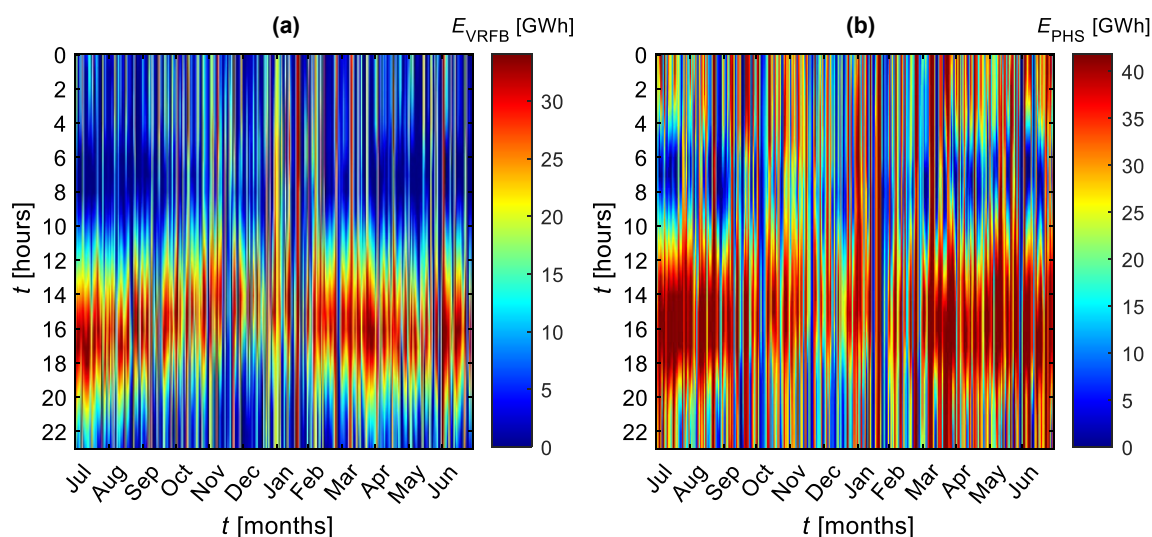


Figure 4.10: Comparison of energy state patterns for case C97.5: (a) VRFB, (b) PHS.

For both VRFB and PHS, charging activities can be predominantly seen in times of PV generation. Discharging is found before and after daylight hours, circling the PV pattern. The maximum energy states can be observed right after the PV peak, showing

that the bulk energy is shifted at this time, as it is for LIB. Nevertheless, several distinctions to the LIB patterns can be seen. In terms of the energy state profiles, remarkably more vertical lines occur, meaning that a certain energy state lasts over the days more often. Therefore, it can be concluded, that more PV energy is shifted inter-day in contrast to LIB, which operates rather intra-day. For a more quantitative evaluation  $t_{cyc}$  is calculated, which verifies this temporal classification: LIB require 0.87 days per full cycle, VRFB and PHS 1.64 and 2.08, respectively.

Through the energy state patterns for PHS and VRFB it further becomes clear that the energy capacity limit is reached less frequently in comparison to LIB. On the contrary, VRFB can be found rather capped by its power capacity. Concurrently, both charging and discharging activities last longer than for LIB. This can be traced back to greater  $EP$ , which also applies for PHS. Finally, a difference in the curvature of the charge pattern is found. As discussed VRFB and PHS take longer to be charged entirely. Thus, if sufficient surplus energy is available, these technologies begin to charge at first. PHS even capture early PV generation which explains a curved nature in the morning hours of the PHS charging profile. Secondary energy shifting as observed for LIB can also be found for VRFB and PHS, albeit in a smaller scale.

In summary it is found that LIB, VRFB and PHS are deployed as short-term storages mainly shifting surplus PV energy. Apart for a minor night to day shift, PV surplus generation is stored during high solar radiation periods by day and shifted to evening and morning hours, where PV generation lacks, and the load level is high at the same time. LIB, having a smaller  $EP$  than VRFB and PHS, shifts energy predominantly intra-day. VRFB and PHS have a growing significance in shifting PV energy inter-day as well.

#### 4.3.4 Long term energy storage

Figure 4.11 shows the wind generation pattern in comparison to the hydrogen storage patterns over the daily and yearly progression. In contrast to the seen PV generation pattern above, wind generation does not follow a daily trend. By the vertical running lines one can observe, that periods of high wind volume mostly last over several days and appear in winter, particularly.

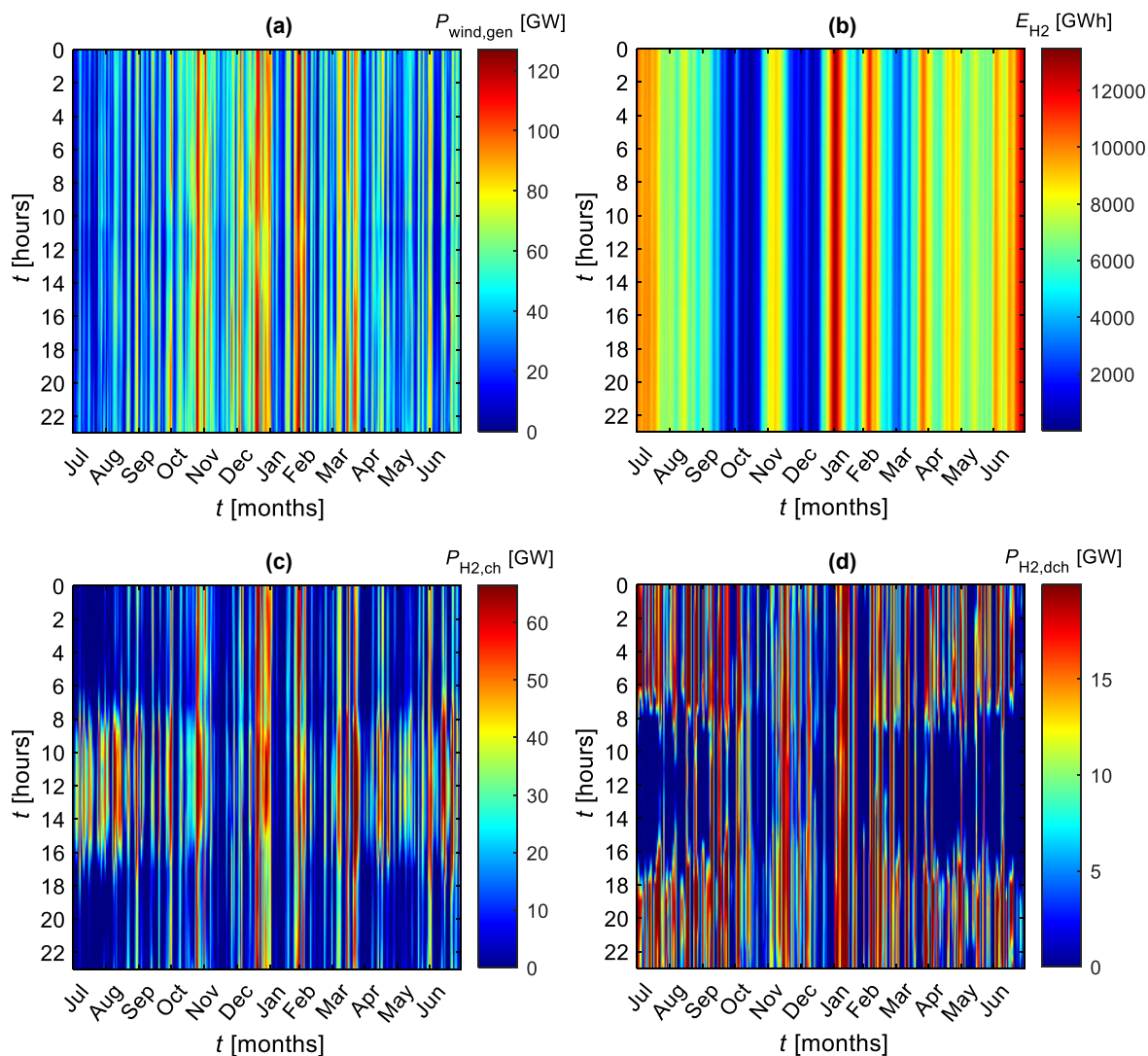


Figure 4.11: Comparison between wind generation pattern and H<sub>2</sub> activities for case C97.5: (a) wind generation pattern, (b) energy state pattern of H<sub>2</sub>, (c) H<sub>2</sub> charging pattern, (d) H<sub>2</sub> discharging pattern.

For the charging behaviour of H<sub>2</sub> a correlation to both wind and PV can be seen. In winter times, the profile is dominated by vertical lines indicating that the charging follows the wind generation. Several greater charging periods are remarkable, for instance in the end of December, which occurs in the wind generation pattern as well. In contrast to winter times, distinct charging activities appear in the other half year. In summer, a great share of charging activity (or the hydrogen production) takes place by day between 8 and 16 o'clock, following the PV generation.

Discharging is basically conducted in two time periods. Firstly, between about 18 and 6 o'clock all over the year, when no PV radiation is available. Discharging in night times might seem unintuitive as the load is low in these times. However, case C97.5 features little dispatchable generator capacities, so that even low loads have to be covered by storages when VRE is not sufficient. Secondly, discharging (or reconverting H<sub>2</sub>) takes

place during daytime between October and February, when the solar radiation is low. This can be seen by the vertical lines in the discharge pattern stretching along a whole day. On the contrary in summer times, when PV radiation is sufficient, low H<sub>2</sub> discharge activities are observed by day.

When looking at the energy state pattern, the long-term character of hydrogen becomes obvious. The wide vertical lines represent periods of high and low energy states, respectively, lasting for longer periods. Hydrogen serves both as a seasonal and monthly storage: The gradually declining state from July and the increasing state from March indicates a seasonal character, shifting VRE surpluses generally from summer to winter. Between October and February, the pattern is marked by several stand-alone lines. These comparatively sudden storage activities come from the mentioned high wind volume periods in winter. In this regard, hydrogen serves rather as monthly storage.

For ACAES a similar deployment can be found, yet not featuring such a strong long-term character as hydrogen. The energy state pattern for ACAES is depicted in Figure 4.12. The corresponding charge and discharge profiles can be found in the appendix A 4.

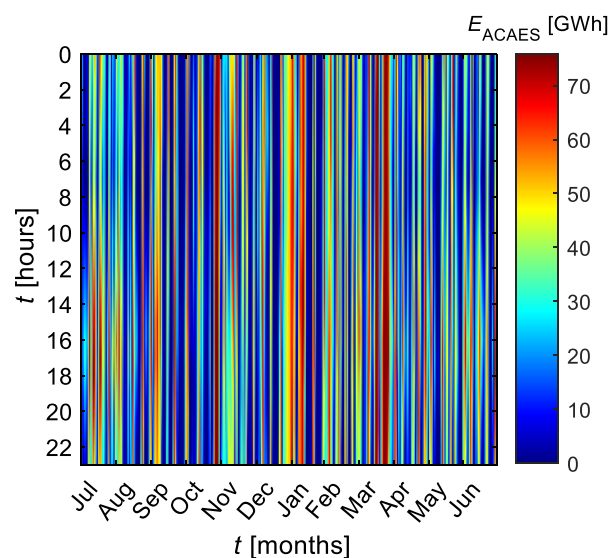


Figure 4.12: ACAES energy state pattern for case C97.5.

While the state of energy pattern for ACAES is also characterized by vertical lines, these appear significant finer. Thus, it becomes apparent that ACAES shifts energy on a long-term scale, albeit for shorter durations than hydrogen. So, hydrogen requires  $t_{\text{cyc}} = 77.72$  days per full cycle on average, ACAES only 4.99.

The charging patterns reveals that both PV and wind generation is stored. Contrary to H<sub>2</sub>, increased charging activities in nightly hours are observed, occurring when wind surplus appears, and the load level is low. The discharge pattern is broadly similar to the one of H<sub>2</sub>, but differences are found in terms of the day-night distribution. So, the bulk share of energy is discharged in the night. Discharge activities by day are rather insignificant and limited to October to December.

In summary it is found that H<sub>2</sub> and ACAES are deployed as long-term storages shifting both PV and wind generation surpluses. PV surplus generation is predominantly charged in summer by day, while the charging activities for wind follow a long-term profile. The energy is shifted to nightly hours all over the year, when load is low but VRE generation still lacks, and on day in winter times, when PV generation is short. Hydrogen serves as a monthly and seasonal storage, while ACAES is rather found to be a weekly storage technology.

#### 4.3.5 Development of storage function over the CO<sub>2</sub> cases

According to the patterns given in the previous section, energy storage technologies are classified in short-term storages that primarily follow PV generation, and long-term storages, for which both PV and wind correlation is found. These classifications are based on the patterns investigated in C97.5 only. A presentation of the patterns for all CO<sub>2</sub> cases would exceed the scope of this work. However, the trend of the days needed for one full storage cycle  $t_{cyc}$ , illustrated in Figure 4.13, gives an impression for the classification over the investigated cases.

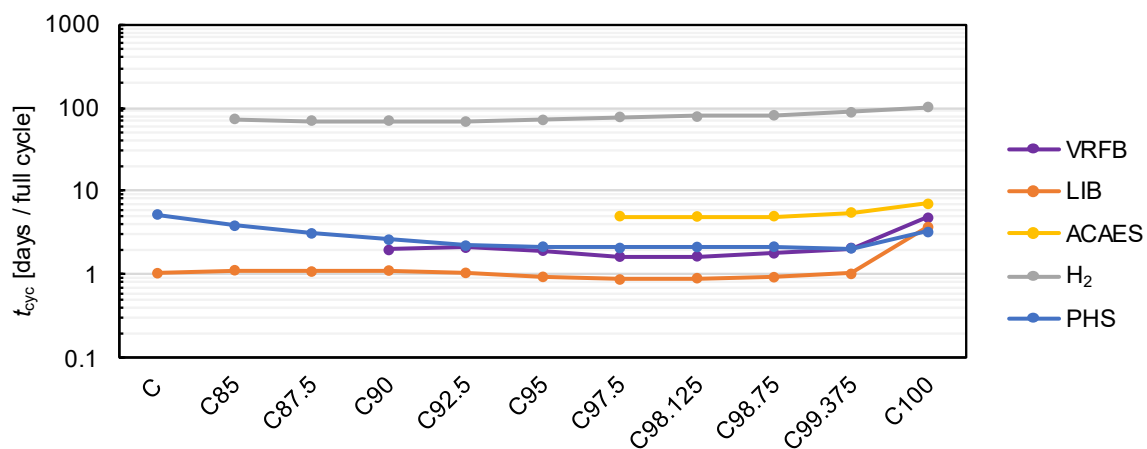


Figure 4.13: Development of the key figure  $t_{cyc}$  for all CO<sub>2</sub> cases.

Basically, the order of  $t_{cyc}$  for the different storage technologies remains the same up to C97.5. Variations can be traced back to the changing energy mix and consequent

diverging *EP* investments for a particular technology. PHS constitutes a special case as these storages already exist, and no further investments are allowed. This could explain the significant fall from C to C90 concerning PHS. LIB feature consistently the greatest short-term characteristics, while approximately charging and discharging every day once, followed by VRFB, that stay in a range of 1.7 to 2.1 days required per full cycle. ACAES is found in a range of 4.99 to 5.5 days per full cycle, thus, is rather seen as a weekly storage. The  $t_{cyc}$  for hydrogen storage range between 68.1 and 88.2 days per full cycle, showing the long-term character.

When approaching C100, a growth of  $t_{cyc}$  for all technologies is seen, indicating the decline of PV deployment as observed in section 4.1. This effect is most outstanding for LIB, why the according LIB patterns are further investigated for case C85 and C100. This allows a broad assessment for the general development of the patterns over the CO<sub>2</sub> cases for all technologies. Figure 4.14 depicts the state of energy pattern for LIB in case C85 and C100.

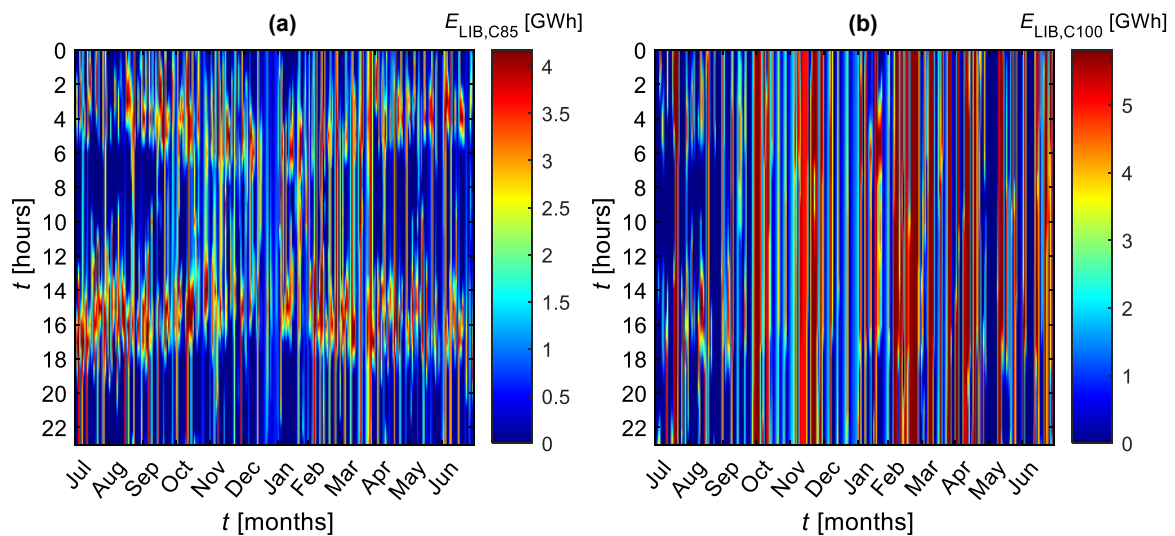


Figure 4.14: Energy state pattern for LIB in case C85 and C100.

The pattern for case C is similar to the one found in C97.5. Even when not as significantly seen, high energy states are found in the afternoon, and in early morning hours. This indicates that the basic storage function of LIB, following PV and a secondary night activity is preserved for lower CO<sub>2</sub> constraints and thus lower VRE shares. On the contrary, the LIB pattern for C100 does not feature a clear PV correlation anymore and is predominantly operating inter-day. This is verified by the strongly increased  $t_{cyc,LIB,C100} = 3.7$  days per full cycle. This development is reasonable in terms of the decreasing PV investment beginning from C97.5.

## 4.4 System cost analysis

Minimizing the system cost is the primary drive that Backbone considers when establishing energy systems. The following section deals with the evaluation of the electricity system model on an economic level comparing the investigated CO<sub>2</sub> cases. In a first step, the total system costs are analysed. Thereafter, a more detailed view is given on the investment cost breakdown.

### 4.4.1 Total system cost

Basically, the total system costs can be divided into fuel and emission costs  $c_{FE}$ , investment costs  $c_{inv}$ , fixed operation and maintenance costs  $c_{FOM}$  and variable operation and maintenance costs  $c_{VOM}$ . The cost breakdown for the respective CO<sub>2</sub> cases is shown in Figure 4.15.

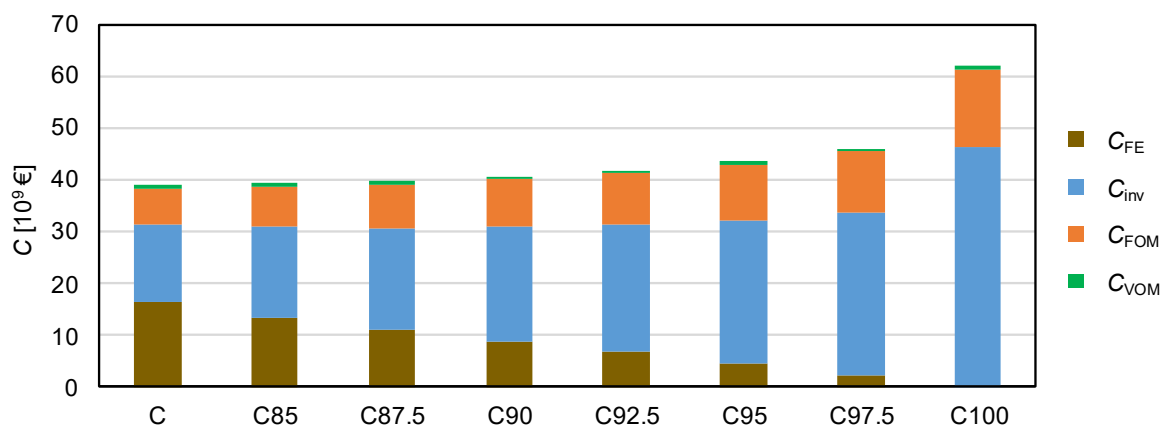


Figure 4.15: Cost breakdown according to the cost types over the CO<sub>2</sub> cases.

In the cost-optimal case C, the total system costs read 38.9 billion €. With increasing limitation of CO<sub>2</sub>, the system costs rise to 45.9 billion € in C97.5 featuring a gently exponential growth. The remaining step from C97.5 to the CO<sub>2</sub> neutral case C100 shows a remarkable leap to 61.8 billion €.

When investigating the cost breakdown, the following characteristics are found. With increasing CO<sub>2</sub> restriction, fuel and emission costs decrease linearly since less fuel can be consumed by GT and the CO<sub>2</sub> emission costs decline as well. On the contrary, investment costs rise significantly. So, these read 15.1 billion € in case C, making a share of 38.7 %, and end up with 46.1 billion € in C100, even making a share of 75.6 % of the total system costs. The FOM costs show a slight growth, while VOM costs make an insignificant share of the total system cost in all cases.

#### 4.4.2 Investment cost

As shown, increasing investment costs are the main reason for the growing system costs. A breakdown of investments costs by technology is shown in Figure 4.16. Up to C97.5, the technology investment expenditures of all technologies except CCGT rise, whose costs decline consistently. In terms of the generation technologies, most investments are spent on offshore wind, followed by PV, onshore wind and CCGT. Regarding storages, hydrogen stands out featuring greater investment costs than LIB, VRFB and ACAES combined, which are summarized in “other ES”. These trends explain the increasing total investment costs until C97.5, and thus system costs. It can be concluded that replacing dispatchable generation by VRE leads to higher costs. On the one hand, more VRE capacities need to be installed to replace a certain amount of dispatchable generation capacity. On the other hand, additional costs occur as storages are needed to shift surplus energy.

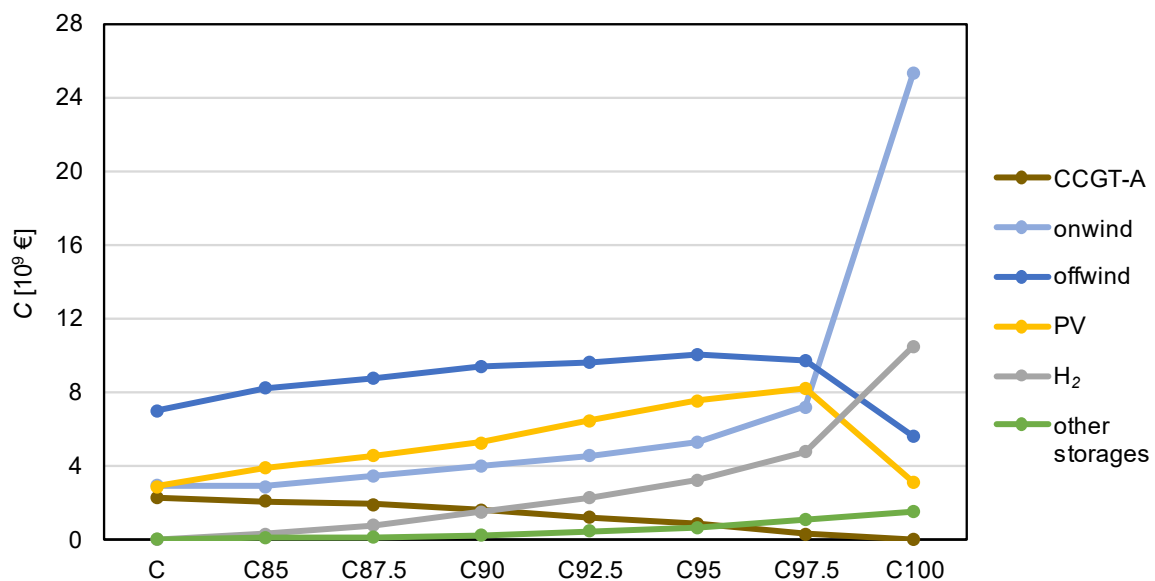


Figure 4.16: Development of investment cost according to technology over the CO<sub>2</sub> cases. “Other storages” include LIB, VRFB and ACAES.

When approaching C100 from C97.5 deviating trends are found. While PV and offshore wind investment costs fall, onshore wind and hydrogen feature a strong increase. Investment costs for onshore wind are even more than tripled, for hydrogen storage more than doubled. These courses are related to the appearance found in section 4.1. When preventing the last remaining GT capacities, PV competitiveness drops, and onshore wind gains huge significance. As shown in section 4.3.4, hydrogen storage correlates strongly with wind activities, why it experiences an increasing deployment when onshore wind usage grows as well.

## 5. Energy storage sensitivity analysis: C97.5

Even when including several references for estimating future states, long-term assumptions are subject to great uncertainties. A sensitivity analysis provides insights in the impact of assumptions on the results and their resilience. For this purpose, several sensitivity scenarios are established in section 3.3, which focus on the deployment of energy storage technologies.

This chapter presents the evaluation for these sensitivity scenarios. The analysis is conducted for the CO<sub>2</sub> case C97.5 since very high shares of renewable energies appear and all storage technologies are used. The actual aimed CO<sub>2</sub> neutral case is not considered, as deviating trends appear when approaching C100 in terms of energy mix, storage deployment and system cost.

Both a technical and an economical parameter variation is conducted. Firstly, deviating CAPEX costs for each storage technology are investigated. In a second step, the impact of the distinct load pattern is explored, considering load pattern developments due to the emerging electrification of the mobility and heat sector. Lastly, the effect of varying storage efficiencies is observed.

### 5.1 Capital expenditures of energy storage technologies

The results for the  $c_{CAPEX}$  scenarios are depicted in Figure 5.1 compared to the case C97.5, which serves as reference. In Figure 5.1 (a) the total storage power capacity investment for the reference case C97.5 can be found, which reads 44.12 GW. Except for the scenarios LIB-20% and VRFB-20%, the total storage power capacity deployment remains approximately similar, when varying the CAPEX costs in the other scenarios by +/-20%. However, the distribution among the storage technologies changes significantly.

When observing the replacement in detail, the same technology competition is found, which is seen in section 4.3. Basically, the storage replacements are related to the order of the key figure  $t_{cyc}$  ( $t_{cyc,LIB} < t_{cyc,VRFB} < t_{cyc,ACAES} < t_{cyc,H2}$ ). Accordingly, the respective technologies compete mainly with their  $t_{cyc}$  "neighbours". For instance, more expensive LIB in scenario LIB+20% result in 2.33 GW additional VRFB capacities, while LIB capacities decline by 2.27 GW. Likewise, when reducing the CAPEX costs of ACAES by 20%, this technology replaces hydrogen and VRFB power capacities partially. Additional 6.69 GW ACAES capacities are seen, and summed VRFB and H<sub>2</sub>

capacities fall by 5.98 GW. Hydrogen primarily competes with ACAES. So, higher hydrogen CAPEX costs follow a replacement by ACAES, lower hydrogen CAPEX costs lead to less ACAES investments.

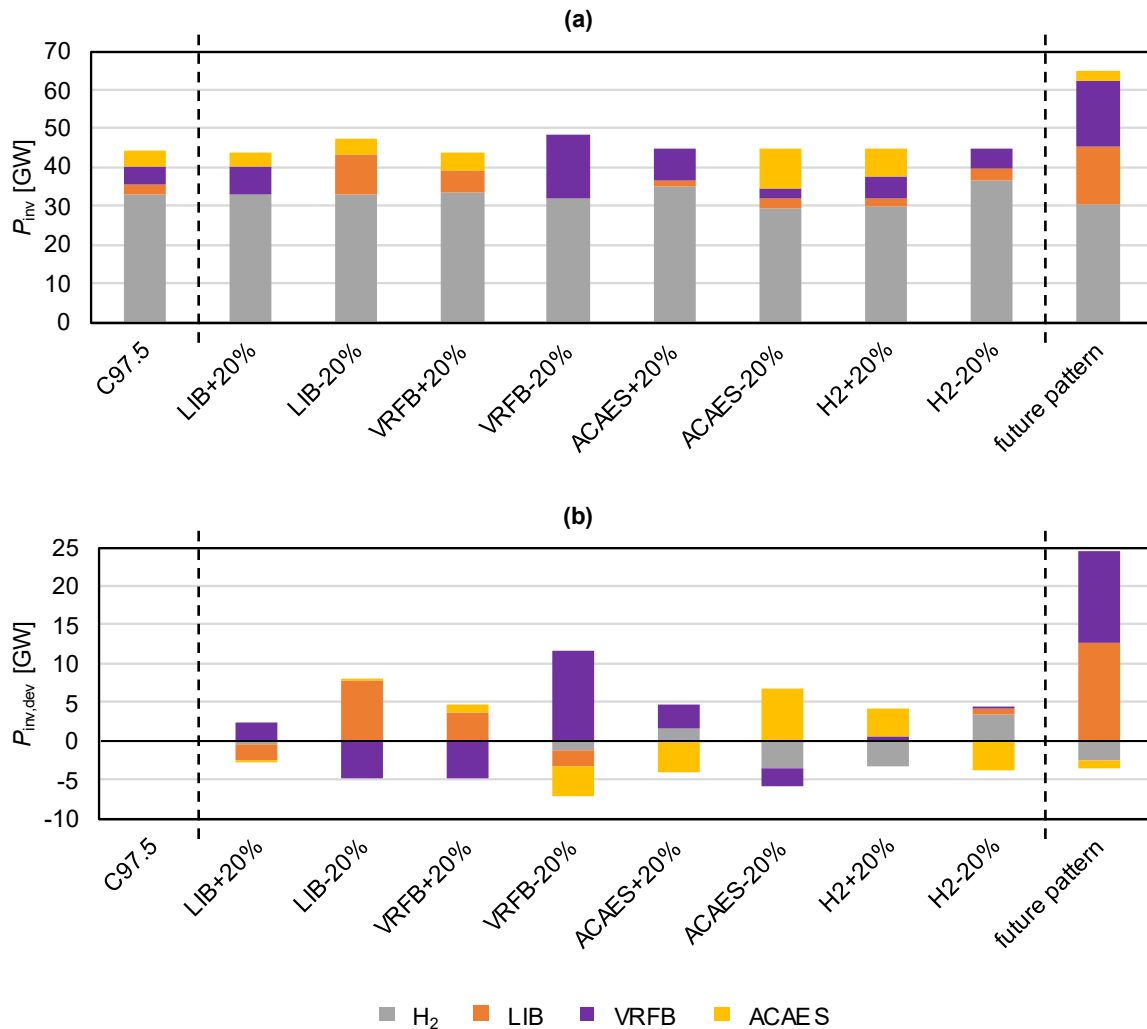


Figure 5.1: Invested storage power capacities for the storage CAPEX scenarios and the future load pattern scenario in comparison to the reference case C97.5: (a) total storage power capacity investments according to the distinct technologies, (b) deviations regarding to the reference case C97.5.

This behaviour seems reasonable since the storage technologies apparently replace their similar functions. For example, LIB compete with VRFB, as both technologies show a strong PV correlation. VRFB further compete with ACAES, as ACAES at least partially show a correlation to PV. Hydrogen is predominantly in competition with ACAES, as both show a connection to wind and PV generation.

Finally, it can be said that the resulting storage technology mix is found highly variable, when investigate CAPEX deviations of 20 % for the respective storage technology. In all according scenarios, except for the ACAES scenarios, at least one storage technology is entirely replaced, so that only three technologies are deployed. A striking

scenario makes VRFB-20%, where VRFB even replace both LIB and ACAES totally. Hydrogen is deployed in any case to a great extent and is not replaced by other technologies in a large extent. This is related to the strong long-term character, that no other in this work investigated storage technology can provide.

## 5.2 Future load pattern

Additional to the varying CAPEX scenarios, the future load pattern scenario is simulated, whose results are also depicted in Figure 5.1. In contrast to the CAPEX scenarios, strikingly increasing storage power capacity investments are found. This is linked to the huge increase of LIB and VRFB investments, seen in Figure 5.1 (b). So, further 16.61 GW and 15.06 GW are installed for VRFB and LIB, respectively. In contrast, ACAES and H<sub>2</sub> capacities decline by a total of 3.52 GW.

This outcome is consistent with the differences of the future load pattern. Significantly greater load is found in the evening hours, which applies especially for the period of November until March, i.e., in winter times. As the PV generation peak occurs around 12 o'clock, a greater need for intra-day energy shift arises. Therefore, the growing investments in LIB and VRFB seems reasonable.

## 5.3 Efficiencies of energy storage technologies

The results regarding the efficiency sensitivity analysis are illustrated in Figure 5.2. Basically, varying the efficiency from a single technology by +/-2.5% does not affect the total deployed storage power capacities significantly, as seen in Figure 5.2 (a). However, the distribution of energy technologies changes. Deviating investments in comparison to the reference case C97.5 can be taken from Figure 5.2 (b). As for the CAPEX scenarios, an enhanced technology replaces its competitive technologies. The replacement characteristics follow the same order as found for the CAPEX cost scenarios. For instance, the increased ACAES efficiency of 2.5% in scenario ACAES+2.5% results in a growing ACAES power capacity of 1.63 GW, while hydrogen and VRFB decline by 1.73 GW in total. When a technology's efficiency is decreased, the opposite behaviour is found. Generally, additional investments of one technology balance out with declining investments of another one, which is why total storage investments remain the same. This does not apply for the H<sub>2</sub> efficiency scenarios, where small deviations in the total deployment are observed.

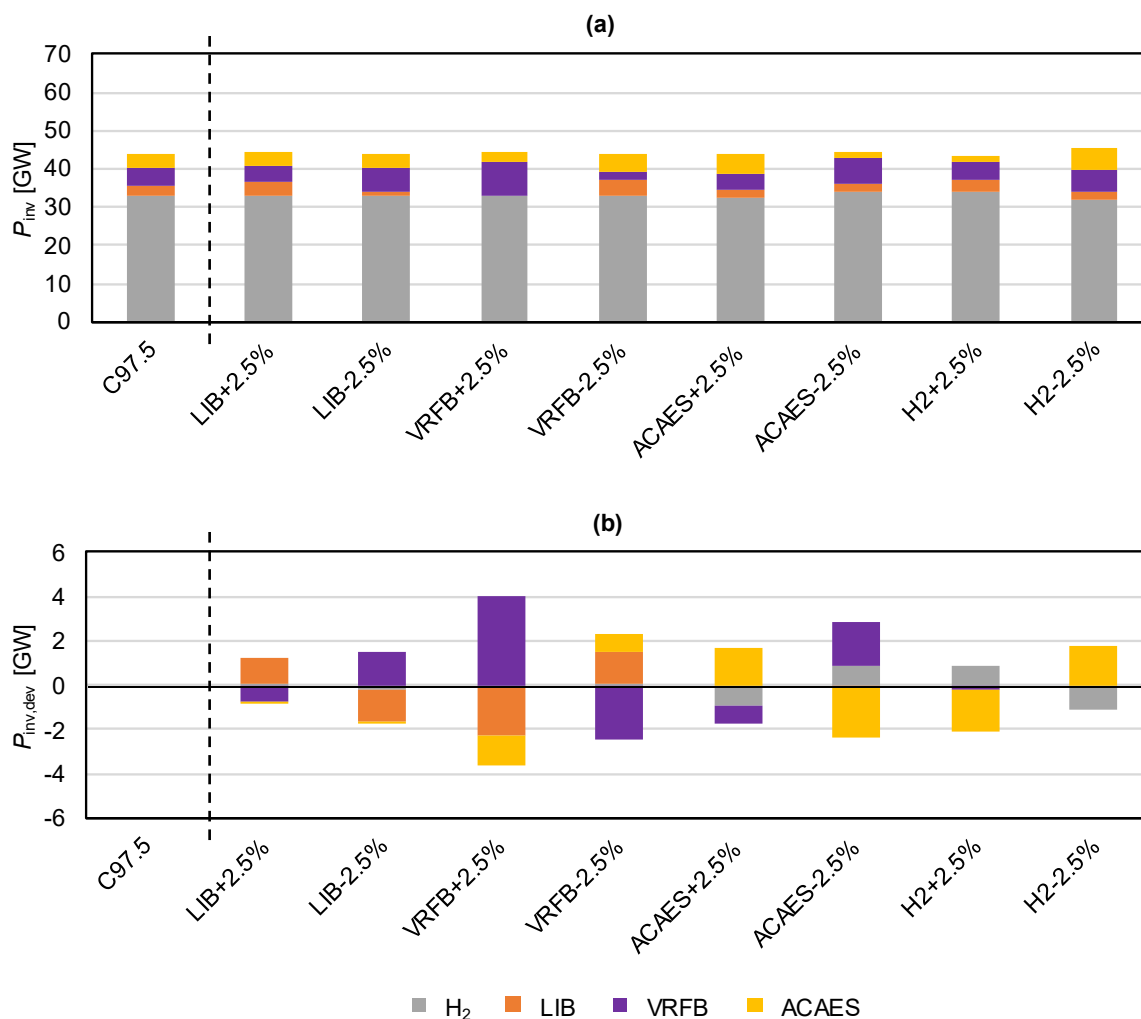


Figure 5.2: Invested storage power capacities for the efficiency scenarios in comparison to the reference case C97.5: (a) total storage power capacity investments according to the different technologies, (b) deviations with regard to the reference case C97.5.

Finally, the resulting storage technology mix is found variable, when investigating efficiency deviations of 2.5 % for a respective storage technology. In contrast to the CAPEX scenarios, no technology is replaced completely, except for LIB in the VRFB+2.5% scenario. Furthermore, hydrogen is used to a great extent in all efficiency scenarios.

A general statement, whether the storage CAPEX or efficiency has a stronger impact on the storage deployment, cannot be made at this point. For this, a more detailed sensitivity analysis must be conducted, exploring the development of these parameters over a greater range. For the limited investigations only, it can be said that the CAPEX cost variation of +/-20 % features a stronger influence on the storage technology mix than the efficiency variation of +/-2.5 %. So, enhancing a technology through decreasing the CAPEX costs by 20 % leads to a greater deployment growth than enhancing it through increasing the efficiency by 2.5 %. For instance, the cost

improvement of LIB in scenario LIB-20% lead to the entire replacement of VRFB. When assuming improved LIB in scenario LIB+2.5% with a 2.5 % increased efficiency, the VRFB investments decline, but are not replaced completely. The same trend can be observed for the other scenarios, accordingly.



## 6. Summary and conclusion

Energy storages may be used to face the challenge of integrating an increasing capacity of variable renewable energies (VRE) within the energy transition. This work is dedicated to the evaluation of promising electrical energy storage technologies. For this purpose, a model of German electricity system in 2050 is established in Backbone, including four innovative storage technologies, namely lithium-ion batteries (LIB), vanadium redox flow batteries (VRFB), adiabatic compressed air energy (ACAES) storages and hydrogen storages. The German network is chosen, as Germany is considered a pioneer in terms of pursuing the energy transition. The network is based on PyPSA-Eur data from 2013, which are modified to reflect a 2050 perspective. Furthermore, several CO<sub>2</sub> emission cases for the German electricity system are investigated based on gradually decreasing emissions compared to 1990.

### 6.1 Key findings

When not imposing any CO<sub>2</sub> emission constraint on the model, the resulting CO<sub>2</sub> emissions read 66.9 million t CO<sub>2</sub>. This is equal to a reduction of 81.7 % compared to the CO<sub>2</sub> emissions of 1990 in the electricity sector. In this case, the renewable energy (RE) share reads 61 %. However, Germany aims at a CO<sub>2</sub> neutral electricity system including a 100 % share of RE generation. While gradually reducing the limit for CO<sub>2</sub> emissions down to the zero-emission case, the deployment of VRE increases and thus periods of surplus generation become more frequent. Concurrently, the energy storage deployment increases exponentially. Noteworthy is the huge leap from case C97.5 to C100. While the RE share increases by the final 4% to a full RE energy mix, the deployment of storage power capacity doubles. This is mainly caused by a large increase of hydrogen storage investments.

It is found that all considered energy storage technologies are used when the electricity system approaches very high shares of RE. The first significant storage investments are found for a RE share of 68 %. While LIB and hydrogen are already deployed from this point, first remarkable amounts of VRFB are used when the RE share exceeds 86 %. Beginning from 96 %, ACAES are deployed as well. Hydrogen takes a more and more dominant position when the RE share grows. Among LIB, VRFB and ACAES a partly competitive behaviour is observed. Moreover, it is found that storage

technologies with greater energy to power ratios are increasingly important at higher shares of RE.

The investigated storage technologies show striking correlations to the VRE generation patterns. Regarding LIB and VRFB (and PHS) storages, a strong correlation to the PV generation pattern is proven. These short-term storage technologies mainly function as daily PV storage and shift surplus PV energy from midday to evening hours. Concerning ACAES and hydrogen, a correlation to both wind and PV generation is seen. These long-term storages charge surplus PV and wind energy, which is then shifted to any time during the year, when VRE generation is lacking. Hydrogen clearly features a stronger long-term character than ACAES.

The system cost analysis reveals a cost increase when CO<sub>2</sub> restrictions are increased, because replacing gas turbines with VRE is more expensive. A significant cost leap occurs while the electric system approaches from 96% to 100% RE share. This is traced back to a huge growth in onshore wind and hydrogen storage investments, that replace the usage of PV and offshore wind generation.

As long-term assumptions are subject to uncertainties, a sensitivity analysis is conducted for the CO<sub>2</sub> case C97.5. Within this analysis, the impact of varying storage capital expenditure costs and varying storage efficiencies are investigated. It is found that the dominant role of hydrogen is broadly independent from the varied parameters. For the other storage technologies, a competitive behaviour is observed again. Especially when varying the CAPEX by +/- 20%, the technology deployment for LIB, VRFB and ACAES changes remarkably. In this case, one technology can even completely replace another. Furthermore, a huge impact on storage deployment is found when using a hypothetical future load pattern, that considers the electrification of the heat and mobility sector. Here, the total storage deployment rises, driven by a significant growth of LIB and VRFB investments.

All in all, it is found that electrical energy storages may be broadly used to face the nature of variable renewable energies. Hydrogen storage has a crucial role, especially for high RE shares. Reaching a CO<sub>2</sub> neutral energy systems leads to a deviating optimal energy mix, increasing VRE curtailment and huge growths of storage deployment and total system costs.

## 6.2 Discussion and outlook

Models are used to represent the reality under certain simplifications. In this thesis, several assumptions are made that may affect the resulting energy systems. The following simplifications are likely to have an impact on the deployment of energy storages, particularly. Germany is assumed to be an island network. However, the energy exchange through the European transmission network balances the fluctuating character of VRE at least in parts. Furthermore, a possible network extension is not considered. Even though the network shifts energy spatially, while storage systems shift energy temporally, a certain competition may occur. Both of these neglects might lead to overestimated storage investments.

Additionally, energy storages do not only shift bulk energy, but can also provide services on the power market, for instance by providing reserve capacities (Sterner and Stadler, 2019, p. 674). The exclusion of this additional market might lead to an underestimation of storage capacity needed. Lastly, ramping characteristics of storages and generators are related to the flexibility they can provide to the energy system. Neglecting ramping characteristics affect the usage of storages and generators as well.

Future work could be generally dedicated to an extension of the established model. The limitations mentioned above should be addressed within the model as they may have crucial impact on the storage deployment. Further attention could be paid to the model when approaching very high shares of RE, where noticeable trends are observed in this work. Also, additional promising storage technologies, such as organic redox flow batteries, could be implemented. Moreover, the inclusion of other flexibility options, such as demand side management or biomass as dispatchable renewable energy, could be considered. The influence of demand side management concerns especially the sensitivity scenario investigating the future load pattern, where storage usage increases significantly. Instead of shifting RE surplus generation, the load of charging electrical vehicles and heat pumps could be shifted temporarily (Gils, 2016). Furthermore, sector coupling could be considered in future work. Finally, a more detailed sensitivity analysis could be useful to reveal the resilience of the results in more detail, especially regarding to the broad deployment of hydrogen.



## Bibliography

- Beuse, M.; Steffen, B. & Schmidt, T. S. (2020): *Projecting the Competition between Energy-Storage Technologies in the Electricity Sector*. In: *Joule*. Vol. 4, no. 10. DOI: 10.1016/j.joule.2020.07.017.
- Böhm, H.; Zauner, A.; Rosenfeld, D. C. & Tichler, R. (2020): *Projecting cost development for future large-scale power-to-gas implementations by scaling effects*. In: *Applied Energy*. Vol. 264, p. 114780. DOI: 10.1016/j.apenergy.2020.114780.
- Boßmann, T. & Staffell, I. (2015): *The shape of future electricity demand: Exploring load curves in 2050s Germany and Britain*. In: *Energy*. Vol. 90, pp. 1317–1333. DOI: 10.1016/j.energy.2015.06.082.
- Bundesamt für Energie (2016): *Wie die Schweizer Druckluft in Tunnel am Gotthard als Energiespeicher nutzen*. In: *Ingenieur.de*, 3 August. URL: <https://www.ingenieur.de/technik/fachbereiche/energie/wie-schweizer-druckluft-in-tunnel-am-gotthard-energiespeicher-nutzen/> (Accessed 06.02.21).
- Bundesregierung (2011): *Deutschlands Energiewende: Ein Gemeinschaftswerk für die Zukunft*. Ethik-Kommission. URL: <https://www.bmu.de/download/deutschlands-energiewende-ein-gemeinschaftswerk-fuer-die-zukunft/> (Accessed 06.02.21).
- Bundesregierung (2020): *Entwurf eines Gesetzes zur Änderung des Erneuerbare-Energien-Gesetzes und weiterer energierechtlicher Vorschriften*. URL: <https://www.bmwi.de/Redaktion/DE/Artikel/Service/Gesetzesvorhaben/gesetz-zur-aenderung-des-eeg-und-weiterer-energierechtlicher-vorschriften.html> (Accessed 13.02.21).
- Bundestag (2020): *Gesetz zur Reduzierung und zur Beendigung der Kohleverstromung und zur Änderung weiterer Gesetze (Kohleausstiegsgesetz)*. Bonn. Bundesgesetzblatt, Jahrgang 2020, Teil I Nr. 37. URL: <http://dipbt.bundestag.de/extrakt/ba/WP19/2587/258735.html> (Accessed 06.02.21).
- Bussar, C.; Stöcker, P.; Cai, Z.; Moraes Jr., L.; Magnor, D. & Wiernes, P., et al. (2016): *Large-scale integration of renewable energies and impact on storage demand in a European renewable power system of 2050—Sensitivity study*. In: *Journal of Energy Storage*. Vol. 6, pp. 1–10. DOI: 10.1016/j.est.2016.02.004.

- BVES (2016a): *Fact Sheet Speichertechnologien: Druckluftenergiespeicher (Compressed Air Energy Storage - CAES)*. Bundesverband Energiespeicher. URL: <https://www.bves.de/technologien-final/> (Accessed 06.02.21).
- BVES (2016b): *Fact Sheet Speichertechnologien: Vanadium Redox Flow Batterien*. Bundesverband Energiespeicher. URL: <https://www.bves.de/technologien-final/> (Accessed 06.02.21).
- Caglayan, D. G.; Weber, N.; Heinrichs, H. U.; Linßen, J.; Robinius, M. & Kukla, P. A., et al. (2020): *Technical potential of salt caverns for hydrogen storage in Europe*. In: *International Journal of Hydrogen Energy*. Vol. 45, no. 11, pp. 6793–6805. DOI: 10.1016/j.ijhydene.2019.12.161.
- Child, M.; Kemfert, C.; Bogdanov, D. & Breyer, C. (2019): *Flexible electricity generation, grid exchange and storage for the transition to a 100% renewable energy system in Europe*. In: *Renewable Energy*. Vol. 139, pp. 80–101. DOI: 10.1016/j.renene.2019.02.077.
- DOE (2020): *Global Energy Storage Database*. U.S. Department of Energy. URL: <https://www.sandia.gov/ess-ssl/global-energy-storage-database-home/> (Accessed 06.02.21).
- European Commission (2019): *The European Green Deal: Communication from the commission to the European Parliament, the European Council, the Council, the European Economic and Social Committee and the Committee of the Regions*. Brussels. European Commission. URL: [https://ec.europa.eu/info/strategy/priorities-2019-2024/european-green-deal\\_en](https://ec.europa.eu/info/strategy/priorities-2019-2024/european-green-deal_en) (Accessed 06.02.21).
- Figgner, J.; Stenzel, P.; Kairies, K.-P.; Linßen, J.; Haberschusz, D. & Wessels, O., et al. (2020): *The development of stationary battery storage systems in Germany – A market review*. In: *Journal of Energy Storage*. Vol. 29, p. 101153. DOI: 10.1016/j.est.2019.101153.
- Fraunhofer ISE (2015): *Current and Future Cost of Photovoltaics: Long-term Scenarios for Market Development,- System Prices and LCOE of Utility-Scale PV Systems. Study on behalf of Agora Energiewende*. Fraunhofer-Institute for Solar Energy Systems. URL: <https://www.agora-energiewende.de/en/publications/current-and-future-cost-of-photovoltaics/> (Accessed 06.02.21).

- Fraunhofer ISE (2020): *Study: Paths to a Climate-Neutral Energy System - The German Energy Transition in its Social Context*. URL: <https://www.ise.fraunhofer.de/en/publications/studies/paths-to-a-climate-neutral-energy-system.html> (Accessed 14.02.21).
- Fraunhofer ISI (2019): *Eine Wasserstoff-Roadmap für Deutschland*. Karlsruhe. Fraunhofer-Institut für System- und Innovationsforschung ISI and Fraunhofer-Institut für Solare Energiesysteme ISE. URL: [https://www.ise.fraunhofer.de/content/dam/ise/de/documents/publications/studies/2019-10\\_Fraunhofer\\_Wasserstoff-Roadmap\\_fuer\\_Deutschland.pdf](https://www.ise.fraunhofer.de/content/dam/ise/de/documents/publications/studies/2019-10_Fraunhofer_Wasserstoff-Roadmap_fuer_Deutschland.pdf) (Accessed 06.02.21).
- Geissbühler, L.; Becattini, V.; Zanganeh, G.; Zavattoni, S.; Barbato, M. & Haselbacher, A., et al. (2018): *Pilot-scale demonstration of advanced adiabatic compressed air energy storage, Part 1: Plant description and tests with sensible thermal-energy storage*. In: *Journal of Energy Storage*. Vol. 17, pp. 129–139. DOI: 10.1016/j.est.2018.02.004.
- Gils, H. C. (2016): *Economic potential for future demand response in Germany – Modeling approach and case study*. In: *Applied Energy*. Vol. 162, pp. 401–415. DOI: 10.1016/j.apenergy.2015.10.083.
- Gils, H. C.; Scholz, Y.; Pregger, T.; Luca de Tena, D. & Heide, D. (2017): *Integrated modelling of variable renewable energy-based power supply in Europe*. In: *Energy*. Vol. 123, pp. 173–188. DOI: 10.1016/j.energy.2017.01.115.
- Gorre, J.; Ortloff, F. & van Leeuwen, C. (2019): *Production costs for synthetic methane in 2030 and 2050 of an optimized Power-to-Gas plant with intermediate hydrogen storage*. In: *Applied Energy*. Vol. 253, p. 113594. DOI: 10.1016/j.apenergy.2019.113594.
- Greim, P.; Solomon, A. A. & Breyer, C. (2020): *Assessment of lithium criticality in the global energy transition and addressing policy gaps in transportation*. In: *Nature communications*. Vol. 11, no. 1, p. 4570. DOI: 10.1038/s41467-020-18402-y.
- Helistö, N.; Kiviluoma, J.; Ikäheimo, J.; Rasku, T.; Rinne, E. & O'Dwyer, C., et al. (2019): *Backbone - An Adaptable Energy Systems Modelling Framework*. In: *Energies*. Vol. 12, no. 17, p. 3388. DOI: 10.3390/en12173388.

- Hörsch, J.; Hofmann, F.; Schlachtberger, D. & Brown, T. (2018): *PyPSA-Eur: An open optimisation model of the European transmission system*. In: *Energy Strategy Reviews*. Vol. 22, pp. 207–215. DOI: 10.1016/j.esr.2018.08.012.
- IPCC (2018): *Global warming of 1.5 °C: An IPCC special report on the impacts of global warming of 1.5°C above pre-industrial levels and related global greenhouse gas emission pathways, in the context of strengthening the global response to the threat of climate change, sustainable development, and efforts to eradicate poverty. Summary for policymakers*. IPCC Switzerland. URL: [https://www.ipcc.ch/site/assets/uploads/sites/2/2018/07/SR15\\_SPM\\_version\\_stand\\_alone\\_LR.pdf](https://www.ipcc.ch/site/assets/uploads/sites/2/2018/07/SR15_SPM_version_stand_alone_LR.pdf) (Accessed 16.02.21).
- Jülch, V. (2016): *Comparison of electricity storage options using levelized cost of storage (LCOS) method*. In: *Applied Energy*. Vol. 183, pp. 1594–1606. DOI: 10.1016/j.apenergy.2016.08.165.
- Jurich, K. (2016): *CO2 Emission Factors for Fossil Fuels*. Umwelt Bundesamt (Climate Change 27/2016). URL: <https://www.umweltbundesamt.de/publikationen/co2-emission-factors-for-fossil-fuels> (Accessed 06.02.21).
- Kaldemeyer, C.; Boysen, C. & Tuschy, I. (2016): *Compressed Air Energy Storage in the German Energy System – Status Quo & Perspectives*. In: *Energy Procedia*. Vol. 99, pp. 298–313. DOI: 10.1016/j.egypro.2016.10.120.
- Knaut, A.; Tode, C.; Lindenberger, D.; Malischek, R.; Paulus, S. & Wagner, J. (2016): *The reference forecast of the German energy transition—An outlook on electricity markets*. In: *Energy Policy*. Vol. 92, pp. 477–491. DOI: 10.1016/j.enpol.2016.02.010.
- Lourenssen, K.; Williams, J.; Ahmadpour, F.; Clemmer, R. & Tasnim, S. (2019): *Vanadium redox flow batteries: A comprehensive review*. In: *Journal of Energy Storage*. Vol. 25, p. 100844. DOI: 10.1016/j.est.2019.100844.
- Moles, C.; Sigfusson, B.; Spisto, A.; Vallei, M.; Weidner, E. & Giuntoli, J., et al. (2014): *Energy Technology Reference Indicator (ETRI) projections for 2010-2050*. Luxembourg. Publications Office. URL: <http://publications.jrc.ec.europa.eu/repository/handle/JRC92496> (Accessed 06.02.21).
- Moser, M.; Gils, H.-C. & Pivaró, G. (2020): *A sensitivity analysis on large-scale electrical energy storage requirements in Europe under consideration of*

- innovative storage technologies*. In: *Journal of Cleaner Production*. Vol. 269, p. 122261. DOI: 10.1016/j.jclepro.2020.122261.
- Pape, C.; Gerhardt, N.; Härtel, P.; Scholz, A.; Schwinn, R. & Drees, T., et al. (2014): *Roadmap Speicher: Speicherbedarf für erneuerbare Energien - Speicheralternativen - Speicheranreiz - Überwindung rechtlicher Hemmnisse*. Fraunhofer-Institut für Windenergie und Energiesystemtechnik, RWTH Aachen, Institut für Elektrische Anlagen und Energiewirtschaft and Stiftung Umweltenergierecht. URL: <https://stiftung-umweltenergierecht.de/projekte/roadmap-speicher/> (Accessed 06.02.21).
- Planet (2014): *Integration von Wind-Wasserstoff-Systemen in das Energiesystem: Abschlussbericht*. Planungsgruppe Energie und Technik GbR, Fachhochschule Lübeck, Fraunhofer-Institut für System- und Innovationsforschung, Institut für Energie und Umwelt and KBB Underground Technologies GmbH. URL: [https://www.planet-energie.de/de/media/Abschlussbericht\\_Integration\\_von\\_Wind\\_Wasserstoff\\_Systemen\\_in\\_das\\_Energiesystem.pdf](https://www.planet-energie.de/de/media/Abschlussbericht_Integration_von_Wind_Wasserstoff_Systemen_in_das_Energiesystem.pdf) (Accessed 06.02.21).
- Sánchez-Díez, E.; Ventosa, E.; Guarnieri, M.; Trovò, A.; Flox, C. & Marcilla, R., et al. (2021): *Redox flow batteries: Status and perspective towards sustainable stationary energy storage*. In: *Journal of Power Sources*. Vol. 481, p. 228804. DOI: 10.1016/j.jpowsour.2020.228804.
- Schill, W.-P. (2020): *Electricity Storage and the Renewable Energy Transition*. In: *Joule*. Vol. 4, no. 10, pp. 2059–2064. DOI: 10.1016/j.joule.2020.07.022.
- Schill, W.-P. & Zerrahn, A. (2018): *Long-run power storage requirements for high shares of renewables: Results and sensitivities*. In: *Renewable and Sustainable Energy Reviews*. Vol. 83, pp. 156–171. DOI: 10.1016/j.rser.2017.05.205.
- Schmidt, O.; Hawkes, A.; Gambhir, A. & Staffell, I. (2017): *The future cost of electrical energy storage based on experience rates*. In: *Nature Energy*. Vol. 2, no. 8. DOI: 10.1038/nenergy.2017.110.
- Schmidt, O.; Melchior, S.; Hawkes, A. & Staffell, I. (2019): *Projecting the Future Levelized Cost of Electricity Storage Technologies*. In: *Joule*. Vol. 3, no. 1, pp. 81–100. DOI: 10.1016/j.joule.2018.12.008.

Sterner, M. & Stadler, I. (2019): *Handbook of Energy Storage: Demand, Technologies, Integration*. 2nd edn. Berlin, Germany. Springer Verlag GmbH. ISBN: 978-3-662-55503-3.

UBA (2020): *Entwicklung der spezifischen Kohlenstoff-Emissionen des deutschen Strommixes*. Umweltbundesamt. URL: <https://www.umweltbundesamt.de/daten/energie/energiebedingte-emissionen#energiebedingte-emissionen-durch-stromerzeugung> (Accessed 16.02.21).

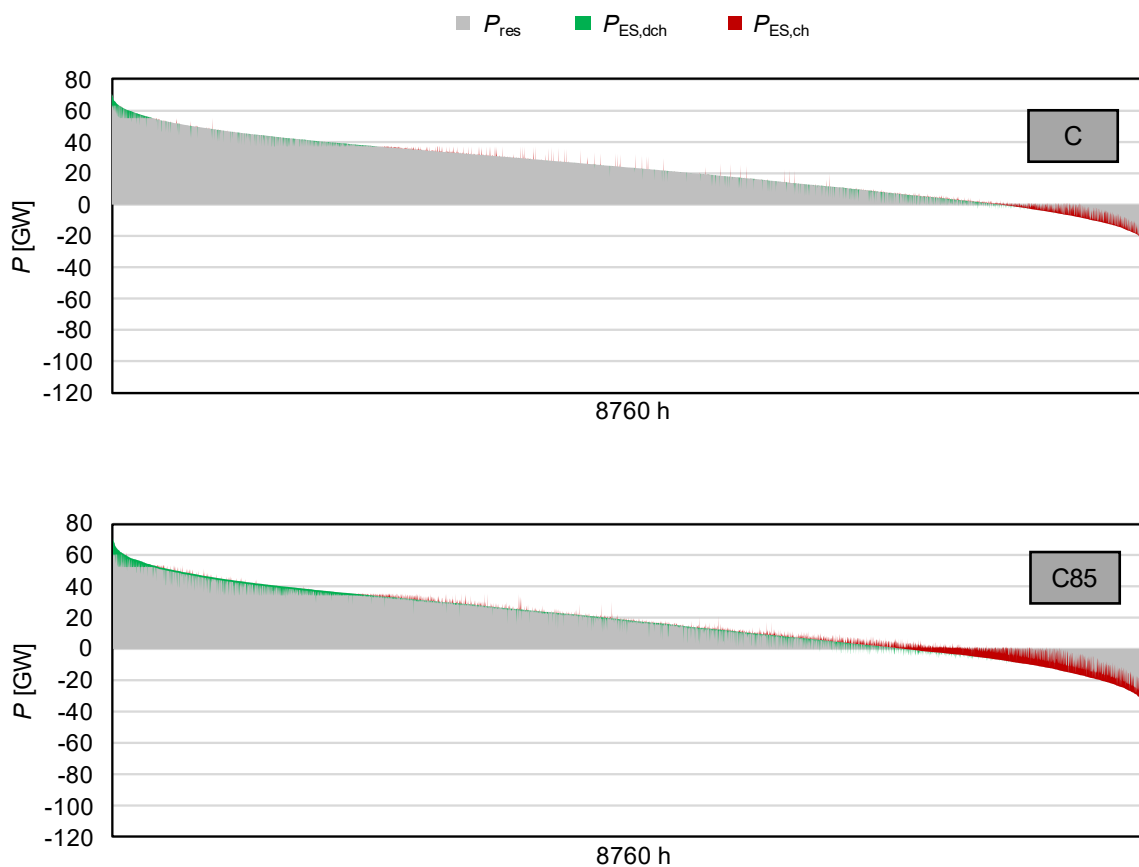
UNFCCC (2015): *Paris Agreement*. United Nations Framework Convention on Climate Change. URL: [http://unfccc.int/files/essential\\_background/convention/application/pdf/english\\_paris\\_agreement.pdf](http://unfccc.int/files/essential_background/convention/application/pdf/english_paris_agreement.pdf) (Accessed 14.02.21).

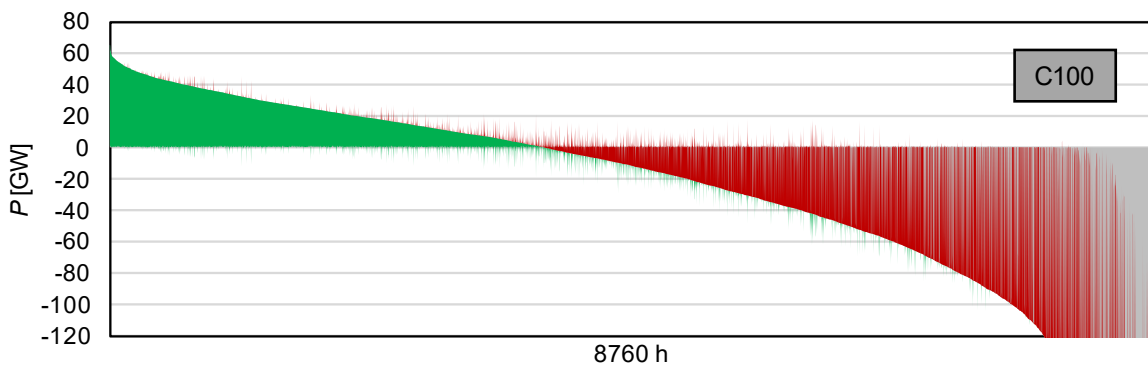
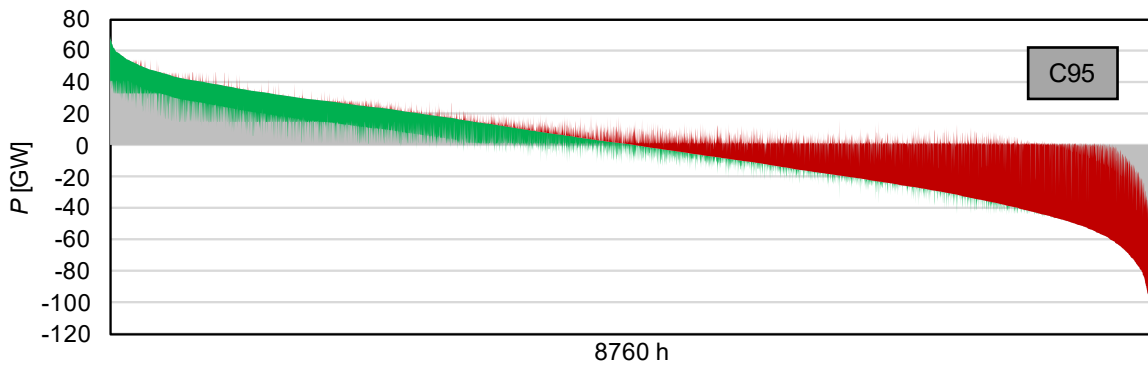
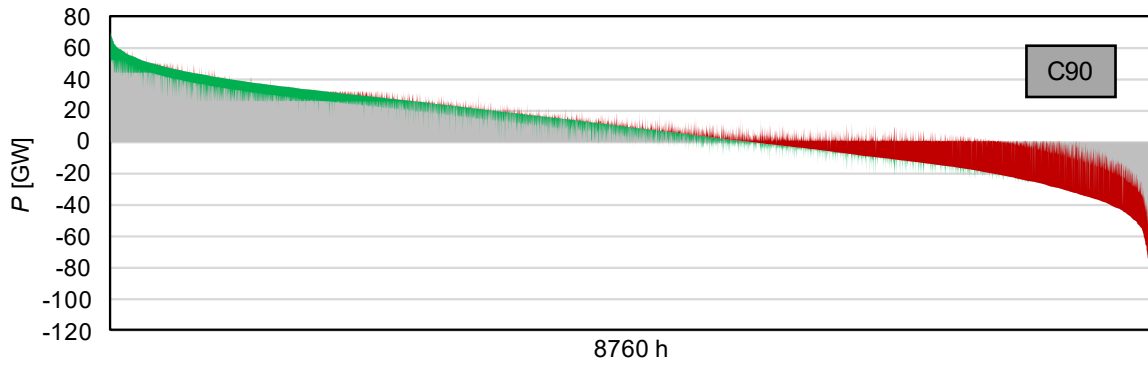
## Appendix

### A 1: Assumptions for initial plant and storage capacities in 2050.

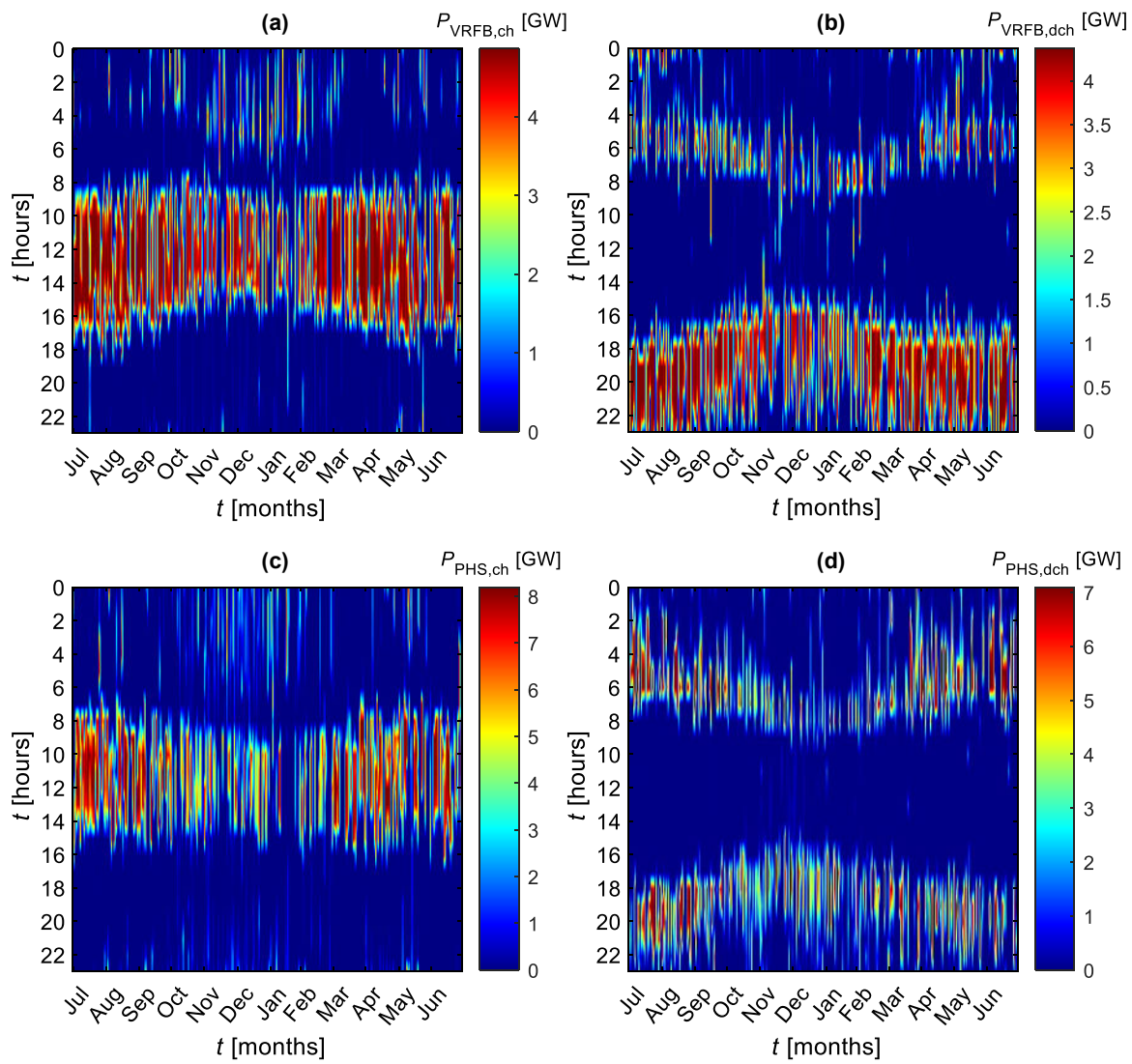
plant	$P_{init}$ [GW]	$C_{FOM}$ [€/(MWa)]	$C_{VOM}$ [€/MWh]	$a$ [a <sup>-1</sup> ]	$\eta$ [-]
CCGT	18.12	23780	4	0.08239	0.50
OCGT	8.04	16340	3	0.08456	0.39
biomass	0.84	100000	0	0.08059	0.47
ROR	2.91	60000	0	0.07031	0.90
PHS	7.10	20000	0	0.07031	0.75
HS	0.19	20000	0	0.07031	0.90

### A 2: Residual load duration curves for chosen CO<sub>2</sub> cases.

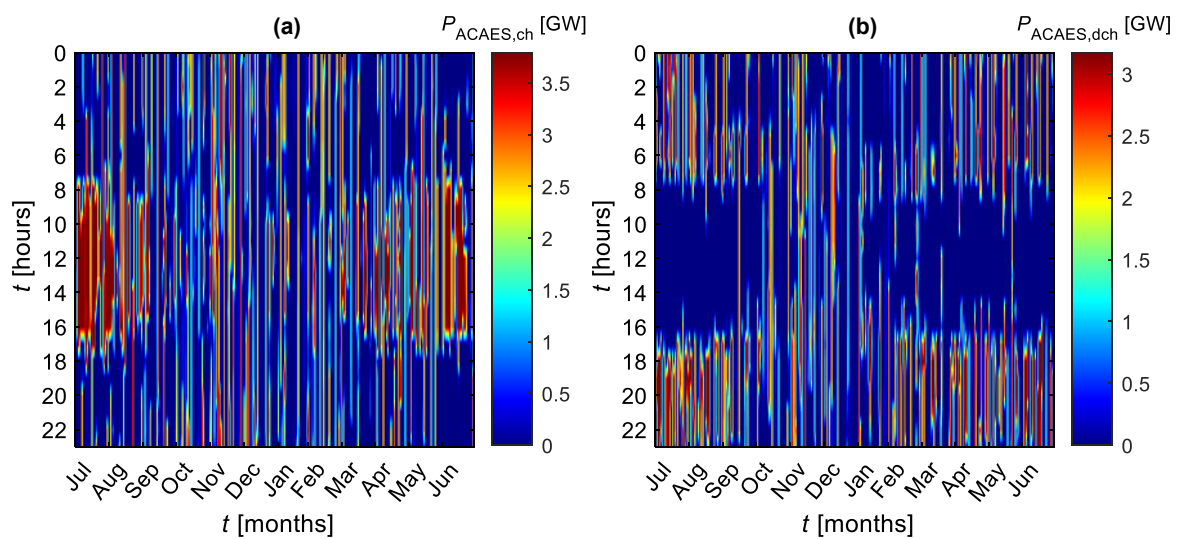




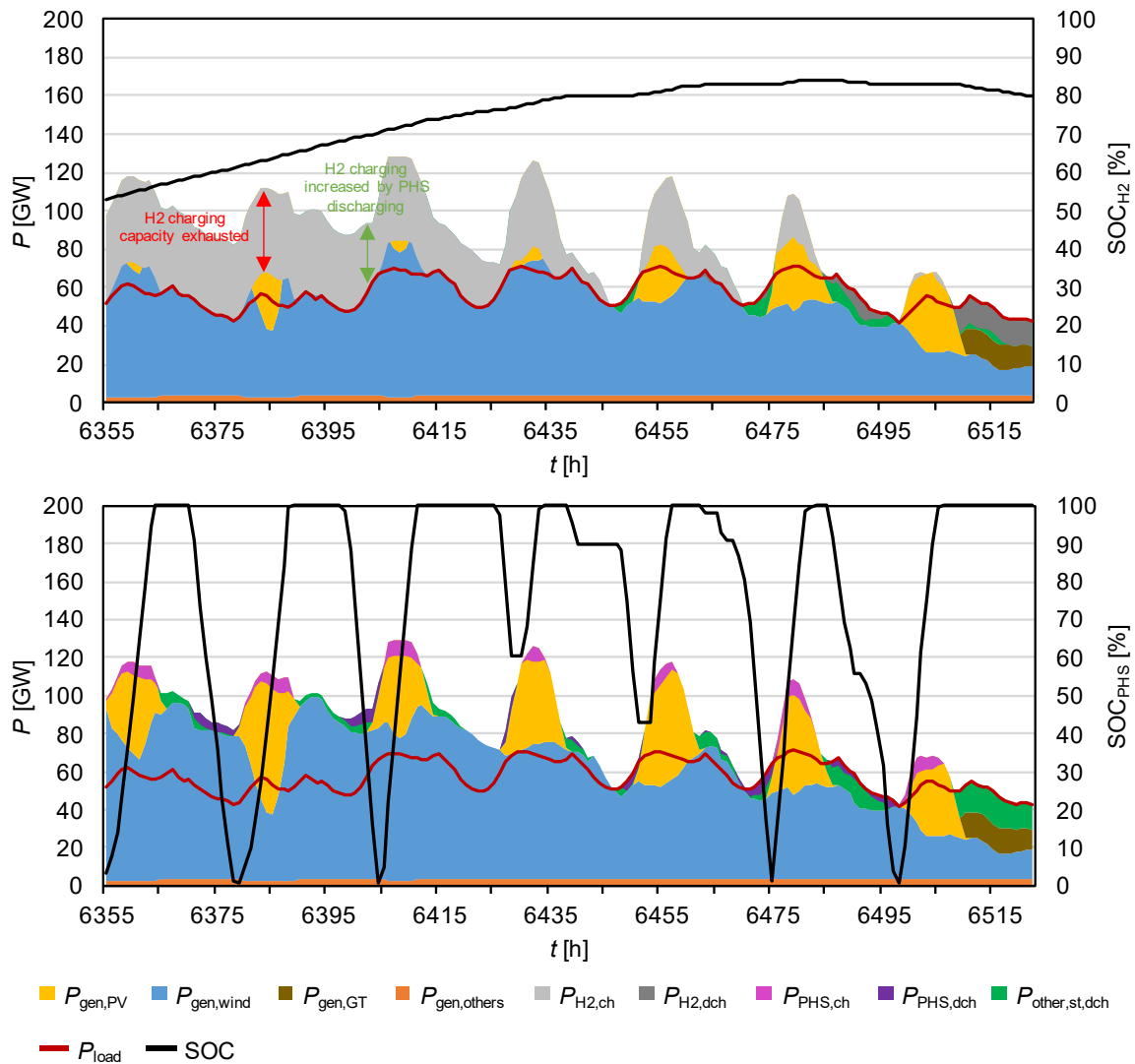
### A 3: Charge and discharge pattern for VRFB and PHS.



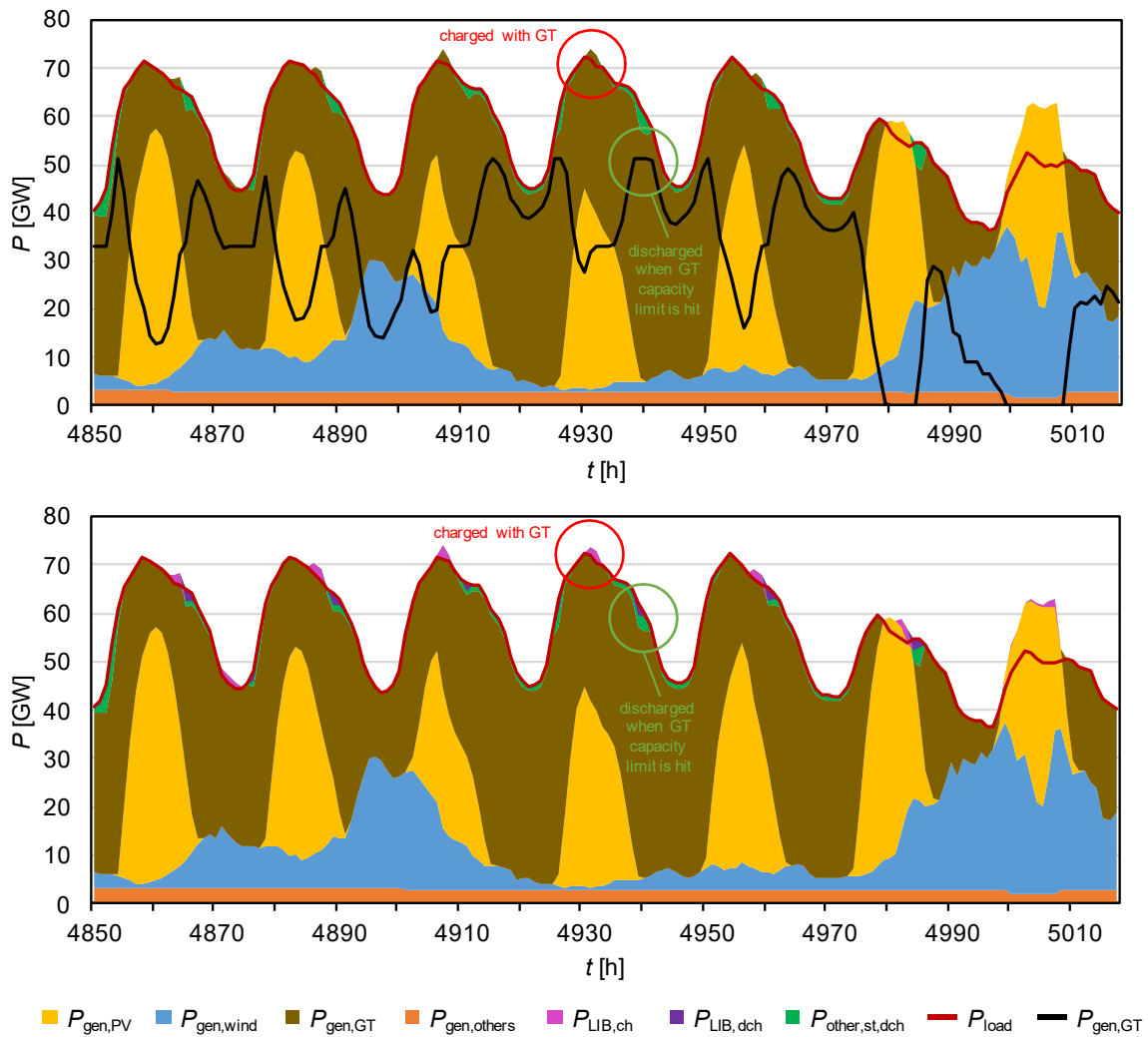
### A 4: Charge and discharge pattern for ACAES.



**A 5:** Exemplary week, extracted from C95, featuring storage communication between PHS and H<sub>2</sub>. PHS is discharged to increase the charging of H<sub>2</sub>. Other generation class includes biomass, ROR and HS.



**A 6:** Exemplary week, extracted from C85, featuring unconventional charging for LIB. Other generation class includes biomass, ROR and HS





## **Eigenständigkeitserklärung**

Hiermit versichere ich an Eides statt, dass ich die vorliegende Arbeit selbständig angefertigt habe. Ich habe außer den im Literaturverzeichnis und im Text genannten Hilfsmitteln keine weiteren verwendet und alle Stellen der Arbeit, die anderen Werken dem Wortlaut oder dem Sinn nach entnommen sind, unter Angabe der Quellen als Entlehnung kenntlich gemacht.

*Jan Mutke*

Jan Mutke

19.02.2021

